N76-2152

ENGINEERING
RESEARCH
INSTITUTE

IOWA STATE
UNIVERSITY
AMES, IOWA

ENGINEERING RESEARCH

ENGINEERING RESEARCH
ENGINEERING RESEARCH
ENGINEERING RESEARCH
ENGINEERING RESEARCH

FINAL REPORT

A STUDY OF TEST SECTION CONFIGURATION FOR SHOCK TUBE TESTING OF TRANSONIC AIRFOILS

William J. Cook
Principal Investigator

June 1978

Submitted to
NASA-Ames Research Center
Grant No. NSG-2152

ISU-ERI-Ames-78336
Project 1233

DEPARTMENT OF MECHANICAL ENGINEERING
ENGINEERING RESEARCH INSTITUTE
IOWA STATE UNIVERSITY AMES

A STUDY OF TEST SECTION CONFIGURATION FOR SHOCK TUBE TESTING OF TRANSONIC AIRFOILS

FINAL TECHNICAL REPORT FOR
NASA - Ames Grant Number NSG-2152*
"High Reynolds Number Transonic Airfoil
Testing in Shock Tubes"
April, 1976 to February, 1978

PRINCIPAL INVESTIGATOR:

William J. Cook
Department of Mechanical Engineering and
Engineering Research Institute
Iowa State University
Ames, Iowa 50011

*The NASA Technical Officer for this grant is Leroy L. Presley, Aerodynamics Branch, NASA Ames Research Center, Moffett Field, California 94035.

ABSTRACT

Two methods are investigated for alleviating wall interference effects in a shock tube test section intended for testing two-dimensional transonic airfoils. The first method involves contouring the test section walls to match approximate streamlines in the flow. The method requires in general that contours be matched to each airfoil tested to produce results close to those obtained in a conventional wind tunnel, but has the distinct advantage of producing flows with known boundary conditions. Data from a previous study and the present study for two different airfoils demonstrate that useful results can be obtained in a shock tube using a test section with contoured walls. The second method involves use of a fixed-geometry slotted-wall test section to provide automatic flow compensation for various airfoils in a manner similar to that provided by slotted-wall test sections used in conventional wind tunnels. The slotted-wall test section developed in the present study exhibits the desired performance characteristics in the approximate Mach number range 0.82 to 0.89, as evidenced by good agreement obtained between shock tube and wind tunnel results for several airfoil flows. The results of the present study further demonstrate that the shock tube can be a useful facility for studying transonic airfoil flows.

TABLE OF CONTENTS

FOREWORD

This report covers the research carried out under NASA-Ames Grant NSG-2152. Part of the results obtained have been reported in a technical paper* which was presented at the 10th AIAA Aerodynamic Testing Conference, San Diego, California, April 19-21, 1978.

*Cook, W. J., Presley, L. L. and Chapman, G. T., "The shock tube as a device for testing transonic airfoils at high Reynolds numbers," AIAA Paper 78-769, 10th AIAA Aerodynamics Testing Conference, San Diego, California, April 19-21, 1978.

NOMENCLATURE

a = Sonic velocity

A_f = Airfoil frontal area

A_s = Slot area, $(n)(s)(x_b)$, Fig. 9

A_{ts} = Test section cross-sectional area, $(H)(W)$ Fig. 9

A_w = Wall area, $(x_b)(W)$, Fig. 9

c = Airfoil chord length

C_p = Pressure coefficient, Eq. (1)

C_p^* = Pressure coefficient at M = 1

d = Slot spacing, Fig. 9

H = Test section height

M = Mach number

M_2 = Shock tube test Mach number, u_2/a_2

n = Number of slots per wall

p = Pressure

Re_c = Chord Reynolds number, $u_2\rho_2 c/\mu_2$

s = Slot width, Fig. 9

t = Time

t' = Time, $t' = 0$ when primary shock is at airfoil leading edge

t_i = Ideal testing time, Fig. 1

u_2 = Region 2 gas velocity relative to airfoil

W = Test section width

x = Distance in flow direction

x_m = Model distance, Fig. 1

y = Distance perpendicular to x

α = Angle of attack

1. INTRODUCTION

There is presently a significant interest in aerodynamic testing facilities with the capacity to generate flows with high Reynolds numbers in the transonic range. In a study reported in [1]* and [2], it was shown that the shock tube has the potential for producing two-dimensional transonic airfoil flows with high chord Reynolds numbers, provided a shock tube of heavy construction is used. Two important aspects must be dealt with if shock tubes are to be used for practical testing of transonic airfoils. The first of these is the quality and duration of the flows produced. The second aspect is the influence of test section walls on the flow field around the airfoil, a problem present to some degree in all transonic testing facilities.

In the shock tube experiments performed at low and intermediate Reynolds numbers, as described in the above-noted study, it was observed that a uniform and turbulent free flow region was produced behind the primary shock. Further, it was observed that steady transonic airfoil flows could be produced within the testing time available in the shock tube, which is typically of the order of milliseconds in the flow regime of interest. Thus, the quality and duration of the test region appears to be adequate for testing transonic airfoils.

For transonic airfoil testing in shock tubes, two methods seemed to offer promise in dealing with the wall interference problem. These are 1) use of contoured test section walls intended to match streamlines

---

*Numbers in brackets refer to references in section 6 of this report.

that occur in free flight, and 2) use of a test section with slotted or perforated walls with adjacent chambers similar to those used in wind tunnels. The first of these two methods was applied to the case of a circular arc airfoil in the above-noted study. In view of the importance of test section wall interference to the testing of airfoils in shock tubes, the present study was undertaken to investigate the matter of test section configuration in more detail. During the course of this investigation, an additional experimental study of airfoil flows in a test section with contoured walls was performed to further assess the contoured-wall testing method. In addition, a slotted-wall test section was developed for use with a shock tube, and transonic flows with intermediate Reynolds numbers were studied for three airfoil profiles to evaluate the performance of the slotted-wall test section.

2. FACILITY DESCRIPTION

2.1 Shock Tube

The shock tube that was used in the research reported in [1] and [2] was used in the present investigation. The driven section has a rectangular cross section 15.2 cm in height and 7.6 cm in width and a length of 10 m. A large dump tank is attached to the downstream end of the driven tube. Mylar diaphragms ranging in thickness from 0.05 to 0.50 mm were used. In lieu of allowing the diaphragms to burst naturally, a diaphragm spear was used in order to allow precise regulation of the driver gas to test gas pressure ratio p_4/p_1 (see Fig. 1), thus permitting accurate control of the test Mach number. Measurement of the primary shock speed and the initial test gas pressure and temperature permitted the flow properties in the test region (region 2, Fig. 1) and hence the flow Mach and Reynolds numbers to be computed. A refinement in the computation of the test region flows was developed during the course of this investigation. This refinement, which accounts in an approximate manner for primary shock wave attenuation, is described in Appendix A (section 8) and was incorporated into the computations for the results presented herein.

2.2 Test Section

The test airfoil was located a distance x_m = 8.6 m from the shock tube diaphragm. See Fig. 1. The test section, 0.46 m in length, extended 0.18 m upstream of the airfoil mid-chord point. The internal dimensions of each end of the test section were matched to the driven tube internal dimensions. The nominal chord length for the airfoil studied was 7.6 cm.

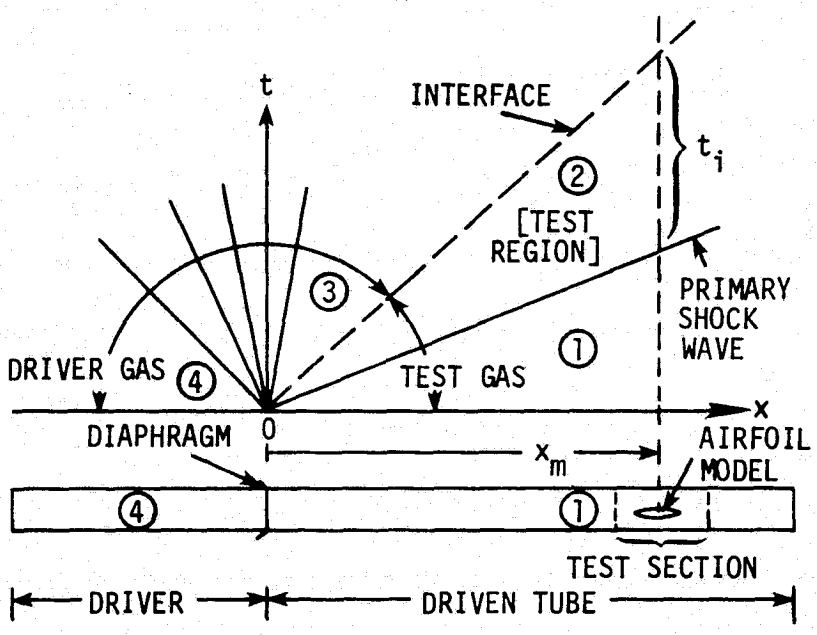

Fig. 1. Shock tube schematic diagram and description of ideal shock tube flow.

This length resulted in a span-to-chord ratio (aspect ratio) of unity and placed the upper and lower test section walls approximately one chord length above and below the airfoil.

The size of the airfoil in relation to the test section size is characterized by two ratios; the test section half-height to the airfoil chord length, H/2c and the airfoil frontal area to the test section cross sectional area, A_f/A_{ts}. The latter ratio is a measure of the blockage due to the presence of the airfoil and must be dealt with by modifying the test section walls. In view of the fact that relatively uniform flows are produced in the shock tube, only the walls above and below the airfoil were modified.

For a nominal chord length of 7.6 cm and a typical 12% thick airfoil, H/2c = 1.0 and A_f/A_{ts} = 0.06 for the shock tube test section. Transonic airfoil testing in most wind tunnels is carried out at smaller values of A_f/A_{ts} and larger values of H/2c. Accordingly, more pronounced wall interference effects than those encountered in wind tunnels would be expected in the present shock tube test section.

At the nominal test Mach number M_2 of 0.85 considered in this study, flows with Re_c value up to 2.0×10^6 could be generated. Using air as both the driver and the test gas, the values of p_1 and p_4 required to produce this Reynolds number were 64.7 and 1380 kPa (0.64 and 13.6 atm), respectively. The Reynolds number was limited by the test section window diameter and thickness. The Reynolds number of the flows that could be generated in the shock tube was large enough to produce turbulent boundary layers upstream of the adverse pressure gradient region on the test airfoils, thus permitting comparisons to be made between results obtained in the shock tube with those obtained in conventional wind tunnels for similar

turbulent airfoil boundary layer conditions. The nominal testing time at $M_2 = 0.85$ was 3.5 ms. This is about 40% of the testing time t_i computed at this test Mach number for an ideal shock tube as described in Fig. 1.

3. CONTOURED-WALL TEST SECTION STUDY

The contoured-wall method of testing requires that approximate two-dimensional stream surfaces for the flow around the airfoil profile be established in some manner. Numerical flow field computation techniques were used to provide the stream surfaces for the present study. These contours were machined into blocks that form the upper and lower walls of the shock tube test section. Although such wall contours may only approximate the real stream surfaces and, therefore, may not exactly reproduce airfoil flows as they would exist in free flight, this method has the distinct advantage of creating experimental flows with known boundary conditions against which results of future transonic computational schemes can be compared.

The flow over a 7.6 cm chord NACA 0012 airfoil at zero angle of attack was studied in the shock tube to further assess the contoured wall method of testing. This airfoil profile was chosen because wind tunnel data are available for comparison purposes. The contour for the test section walls was computed using a transonic computer code [3]. Figure 2 shows the test section wall contour and the corresponding axial position of the airfoil.

Two methods were employed to study the airfoil flow. Schlieren photography provided a means of examining the airfoil flow development and steady flow patterns in detail. The other method consisted of measuring the pressure variation with respect to both time and position on the airfoil.

Figure 3 presents a series of schlieren photos taken of the flow over the 0012 airfoil at various times after primary shock wave arrival.

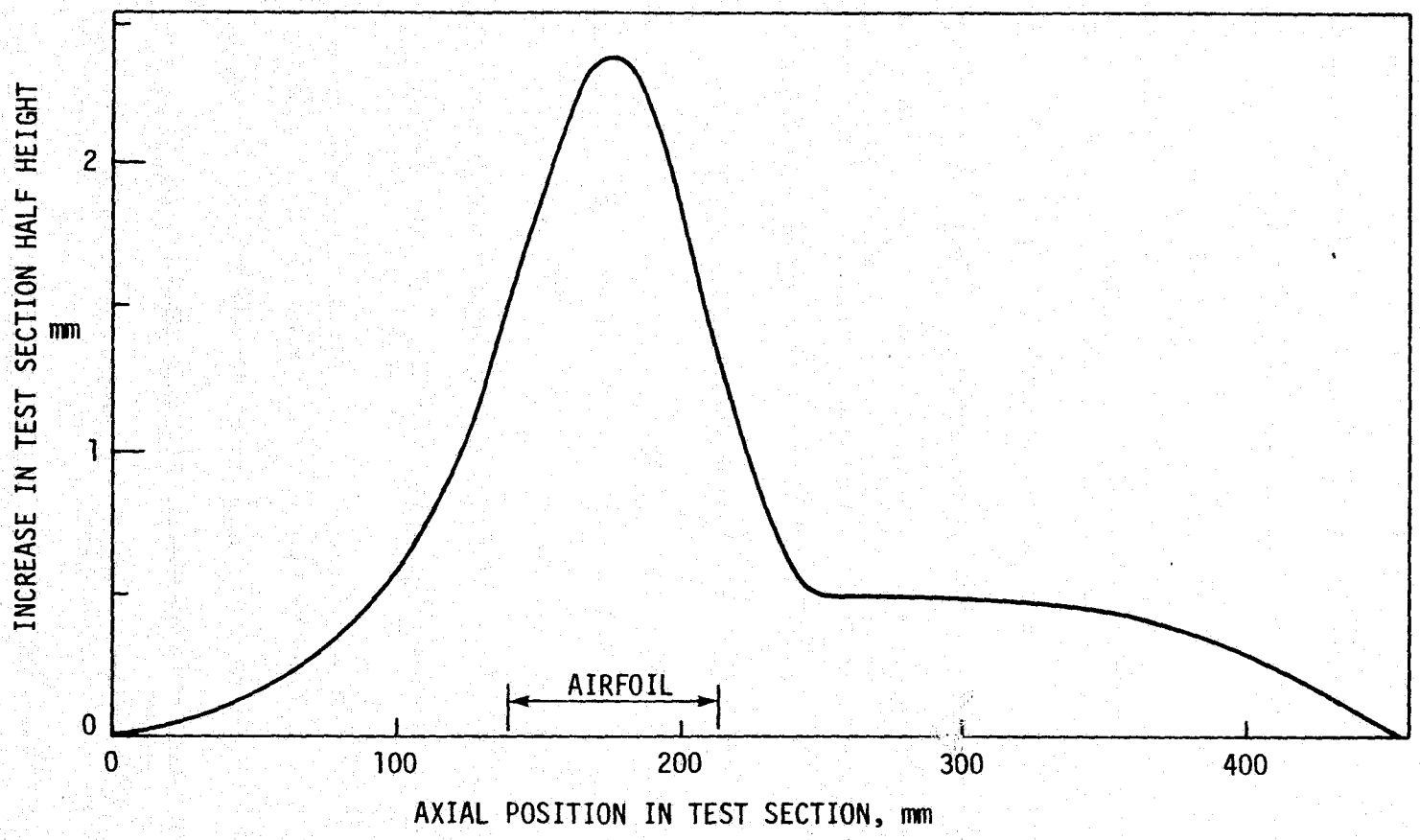

Fig. 2. Shock tube test section wall contour for NACA 0012 airfoil. c = 7.6 cm, H/2c = 1, M = 0.85

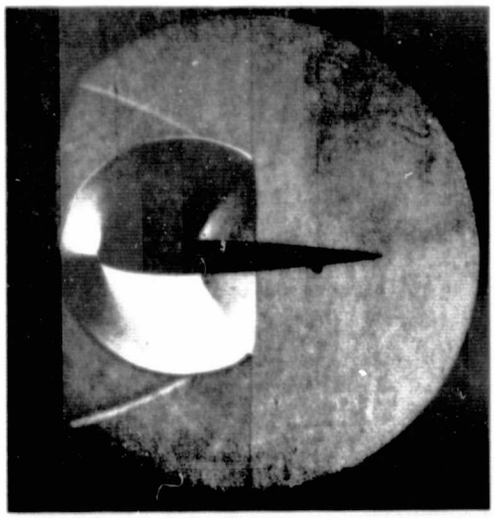

(a) t' = 0.064 ms

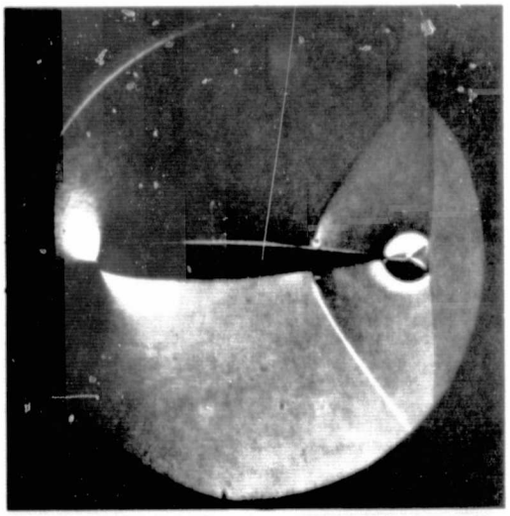

(b) t' = 0.134 ms

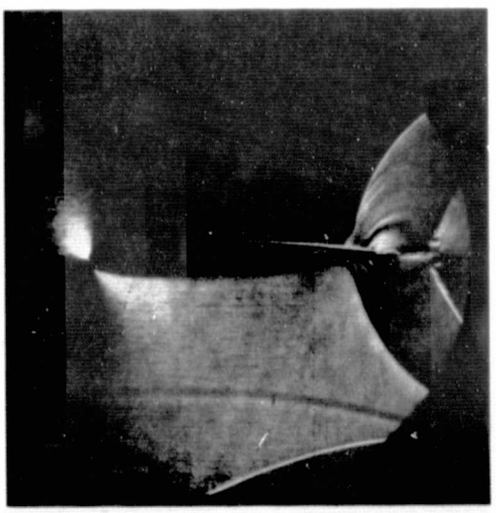

(c) t' = 0.22 ms

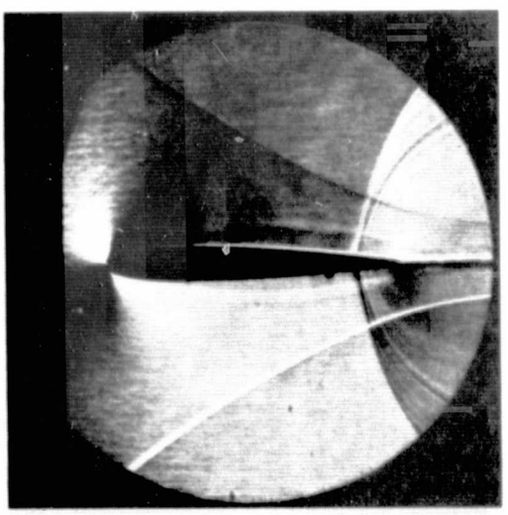

(d) t' = 0.30 ms

Fig. 3. Schlieren photos of flow development for the NACA 0012 airfoil. M = 0.85 contoured test section walls. M_2 = 0.85, c = 7.6 cm, $Re_c = 2 \times 10^6$, $\alpha = 0$.

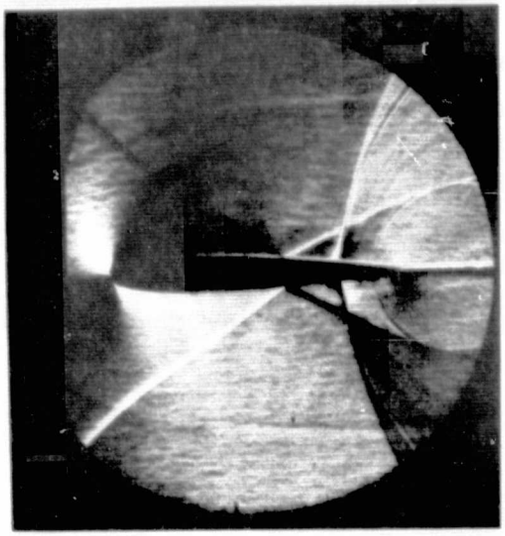

(e) t' = 0.40 ms

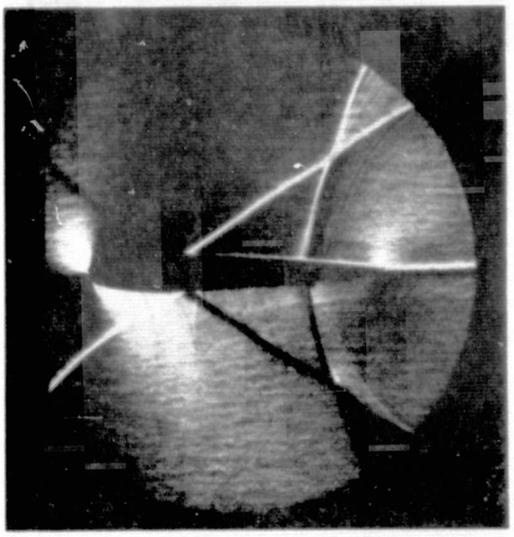

(f) t' = 0.50 ms

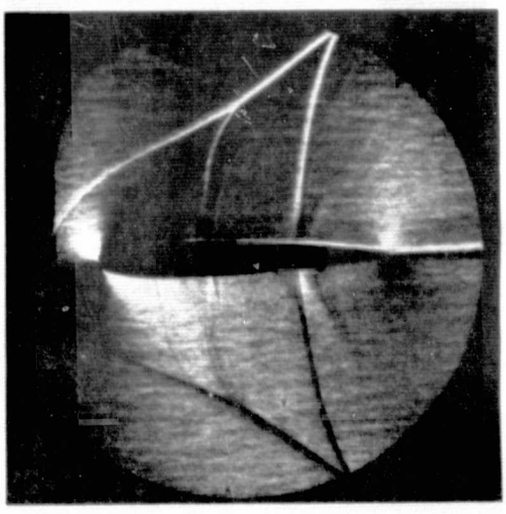

(g) t' = 0.60 ms

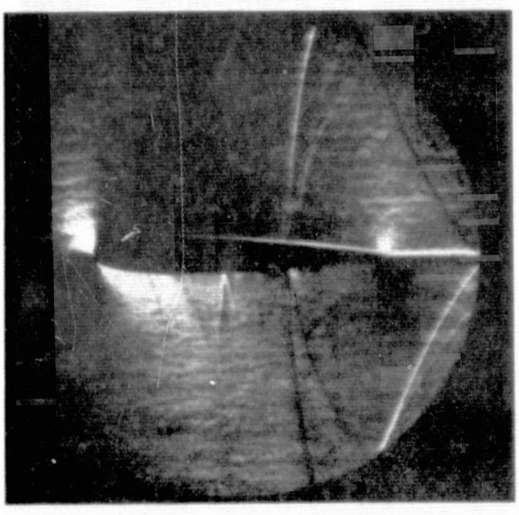

(h) t' = 0.70 ms

Fig. 3. Continued.

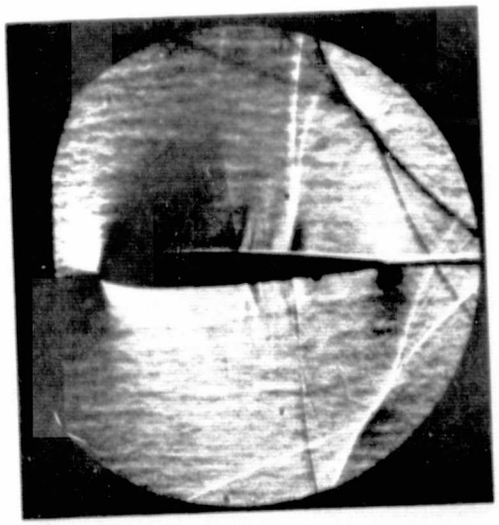

(i) t' = 0.80 ms

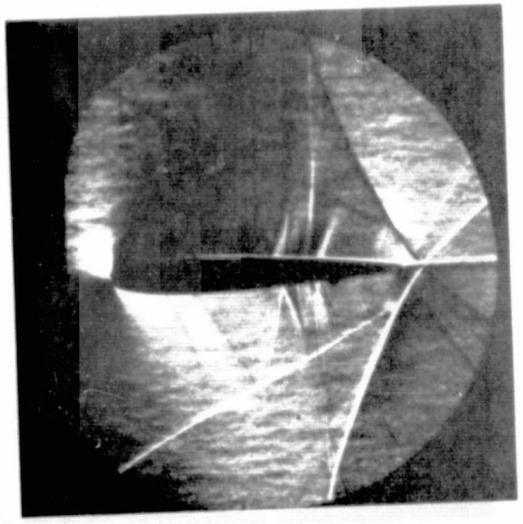

(j) t' = 0.90 ms

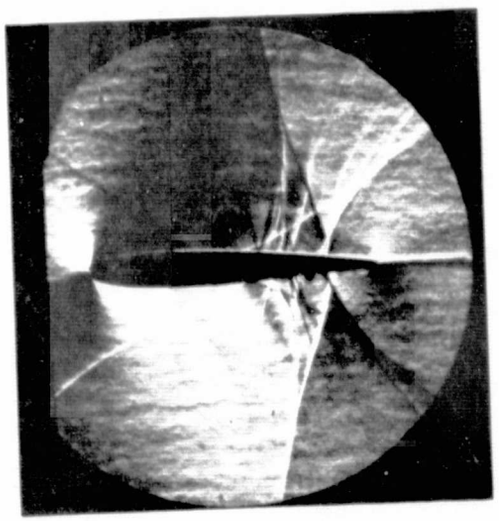

(k) t' = 1.0 ms

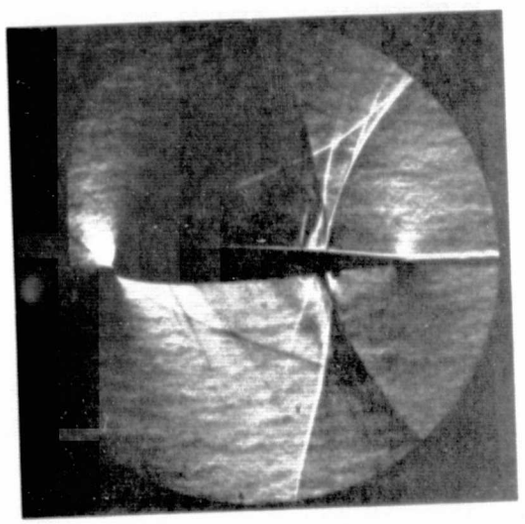

(l) t' = 1.1 ms

Fig. 3. Continued.

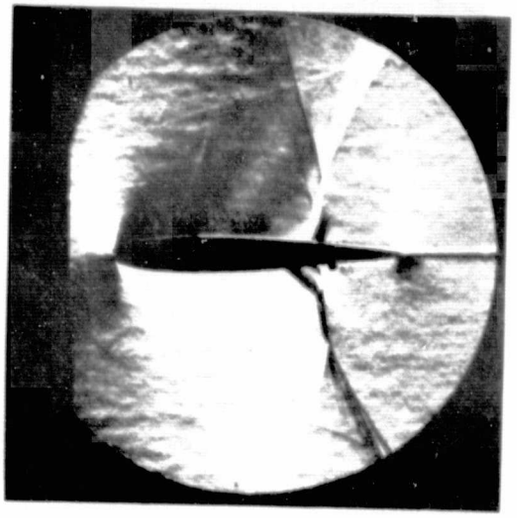

(m) t' = 1.2 ms

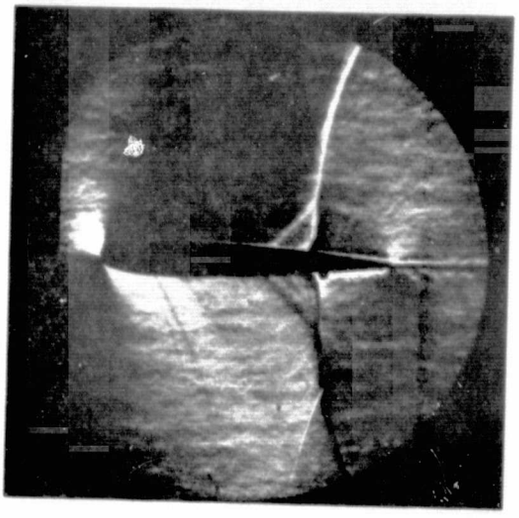

(n) t' = 1.3 ms

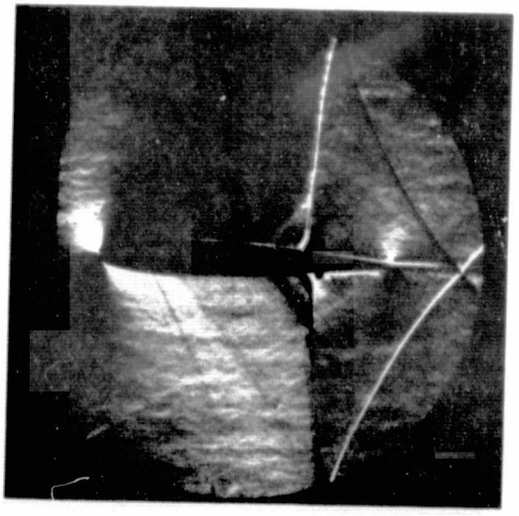

(o) t' = 1.5 ms

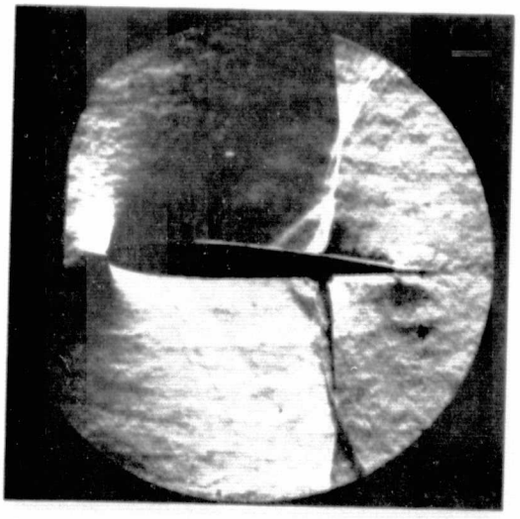

(p) t' = 1.9 ms

Fig. 3. Continued.

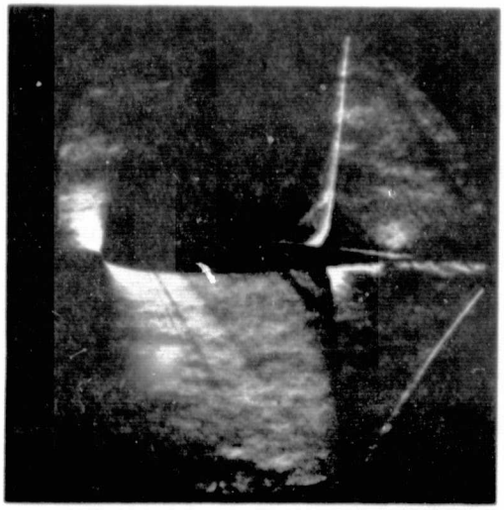

(q) t' = 2.1 ms

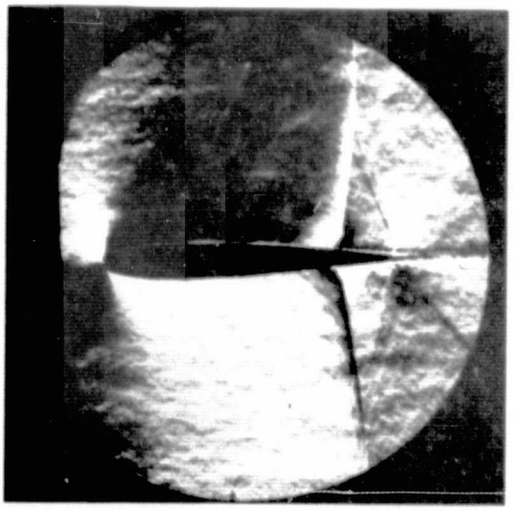

(r) t' = 2.3 ms

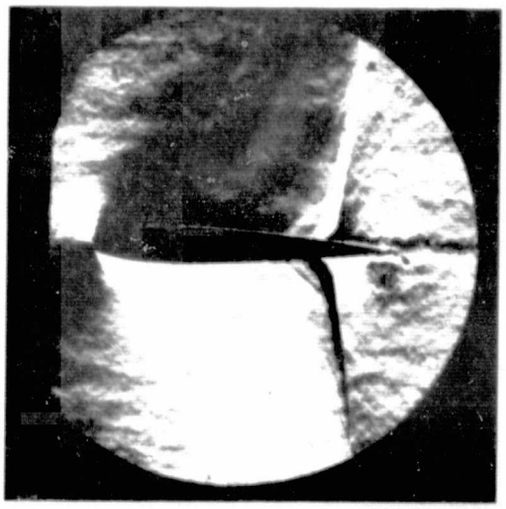

(s) t' = 2.5 ms

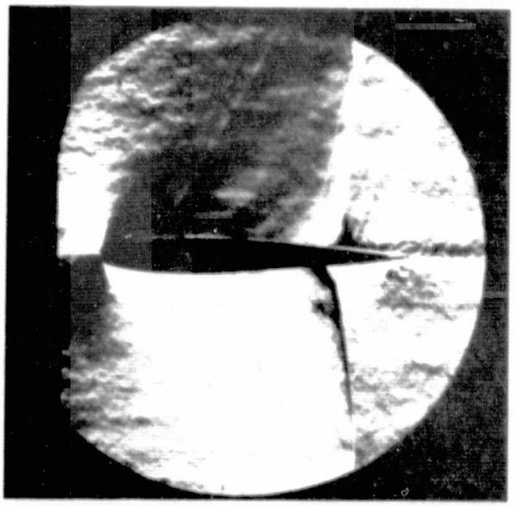

(t) t' = 3.0 ms

Fig. 3. Concluded.

In the photos, $t' = 0$ when the shock wave is at the airfoil leading edge. The values of the test Mach number M_2 and the chord Reynolds number Re_c for the flows shown in Fig. 3 are 0.85 and 2×10^6, respectively. The photos provide a visual description of the flow development. The circular wave in Fig. 3(a) is a reflected wave that forms as the primary shock interacts with the airfoil. This wave grows with time and is reflected from the upper and lower test section walls between the times noted in Figs. 3(b) and 3(c), producing wave patterns that become increasingly complex as multiple reflections occur and the flow develops. In Fig. 3(e) the shock wave on the airfoil begins to form and is essentially established at $t' = 2.3$ ms, Fig. 3(r). Figures 3(s) and 3(t) show the final steady flow patterns. A fine-structured turbulence is first evident in Figs. 3(c) and 3(d), and as time increases a different structure of turbulence is observed in the photos. This appears to stabilize at $t' \simeq 1.5$ ms. This turbulence is due to the presence of the turbulent sidewall boundary layer on the windows of the test section. Computations [1] indicate that by the end of the testing time, each of the two sidewall boundary layers covers 23% of the span of the airfoil for the case $M_2 = 0.85$ and $Re_c = 2 \times 10^6$. However, since in turbulent boundary layers the major portion of the velocity deficit is near the wall, no large velocity gradients were indicated in the spanwise direction for the center portion of the span.

The steady shock wave profiles like those in Figs. 3(s) and 3(t) provide a quantitative means of comparing the flows observed in the shock tube tests for the 0012 airfoil with those observed in a wind tunnel. Figure 4 presents a comparison of shock wave profiles for the NACA 0012 airfoil observed in the contoured wall test section at $Re_c = 2 \times 10^6$

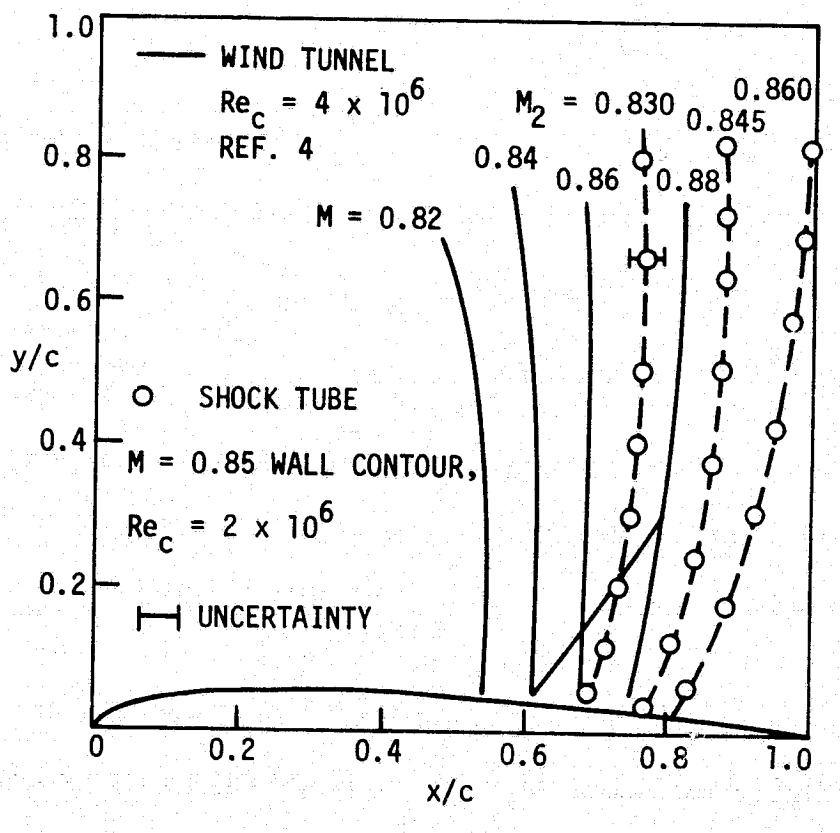

Fig. 4. Comparison of shock wave profiles for NACA 0012 airfoil. $\alpha = 0$.

and profiles obtained from schlieren photos taken in wind tunnel tests of this airfoil conducted by Stivers [4] in the NASA Ames Research Center 2 x 2 ft transonic wind tunnel at $Re_c = 4 \times 10^6$ using a 15.2 cm chord length model. The shock profiles for the shock tube tests in Fig. 4 are seen to lie downstream of those observed in the wind tunnel.

A separate NACA 0012 airfoil with a chord length of 7.6 cm was used in the pressure distribution study. Six Kulite pressure transducers* were mounted internal to the model and sensed the surface pressure at various values of x/c through short small-diameter holes drilled to the airfoil surface at midspan.

Figure 5(a) presents tracings of the oscilloscope records, pressure change vs t', for a typical run for the six gages. The location of each gage is noted in the figure in terms of x/c. The records indicate that steady pressure values were attained by t' = 2 ms and that essentially steady flow existed until at least the termination of the nominal testing time, 3.5 ms. The tracing for the gage response at x/c = 0.49 shows the limits of a highly-oscillatory signal which was apparently due to the interaction of turbulence at that location with the passage leading to the pressure transducer.

The local steady pressure p on the airfoil surface is $p_1 + \Delta p$, where Δp is determined from the time-steady segments of oscilloscope records like those in Fig. 5(a). In the pressure coefficient expression

$$C_p = \frac{p - P_\infty}{1/2\rho_\infty u_\infty^2} = \frac{(P/P_\infty) - 1}{\gamma M_\infty^2/2} \tag{1}$$

*Model LQL-080-25, Kulite Semiconductor Products, Inc., Ridgefield, N.J.

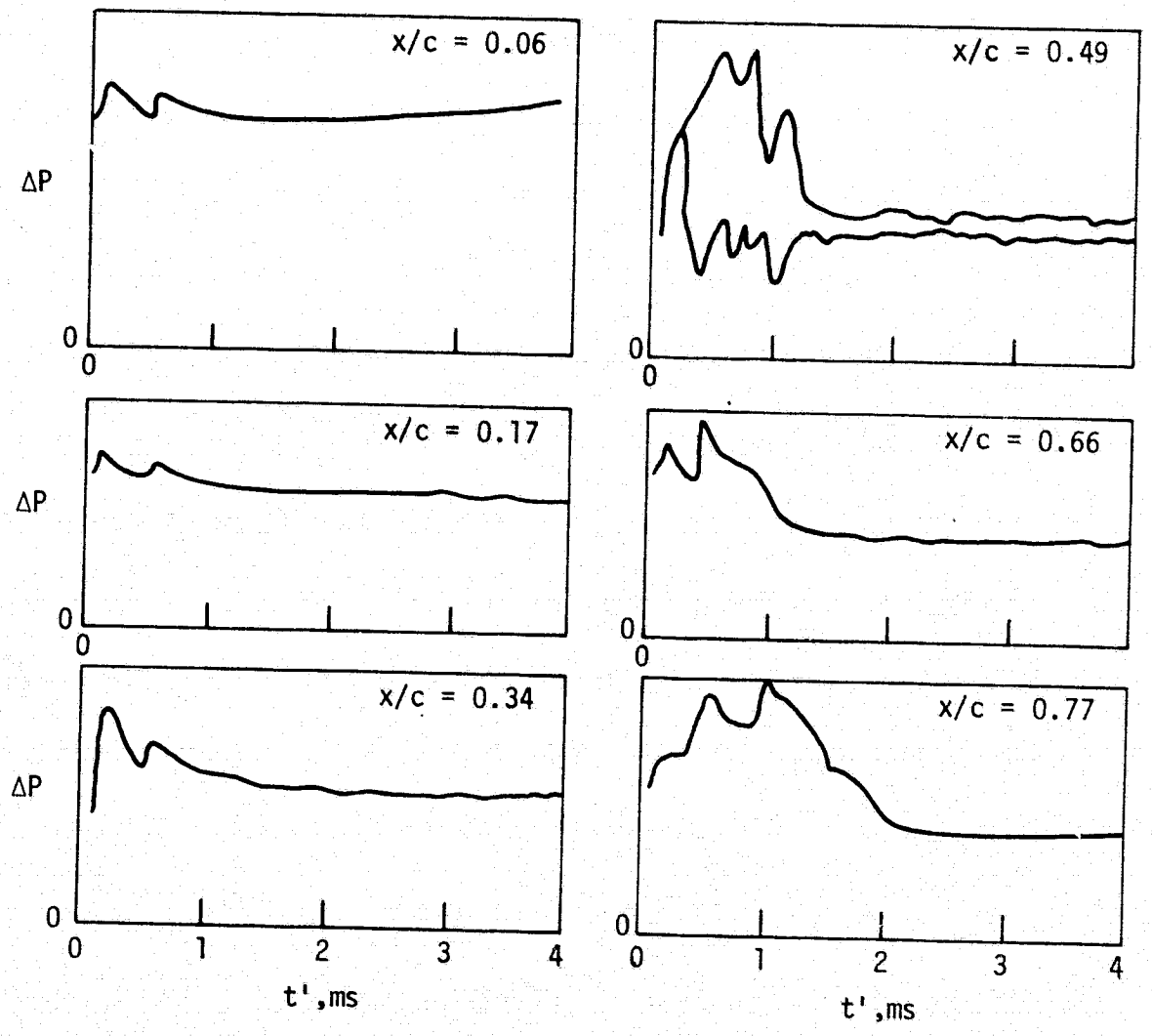

(a) Typical transducer response records.

Fig. 5. Results obtained from pressure measurements. NACA 0012 airfoil. M = 0.85 contoured test section walls.

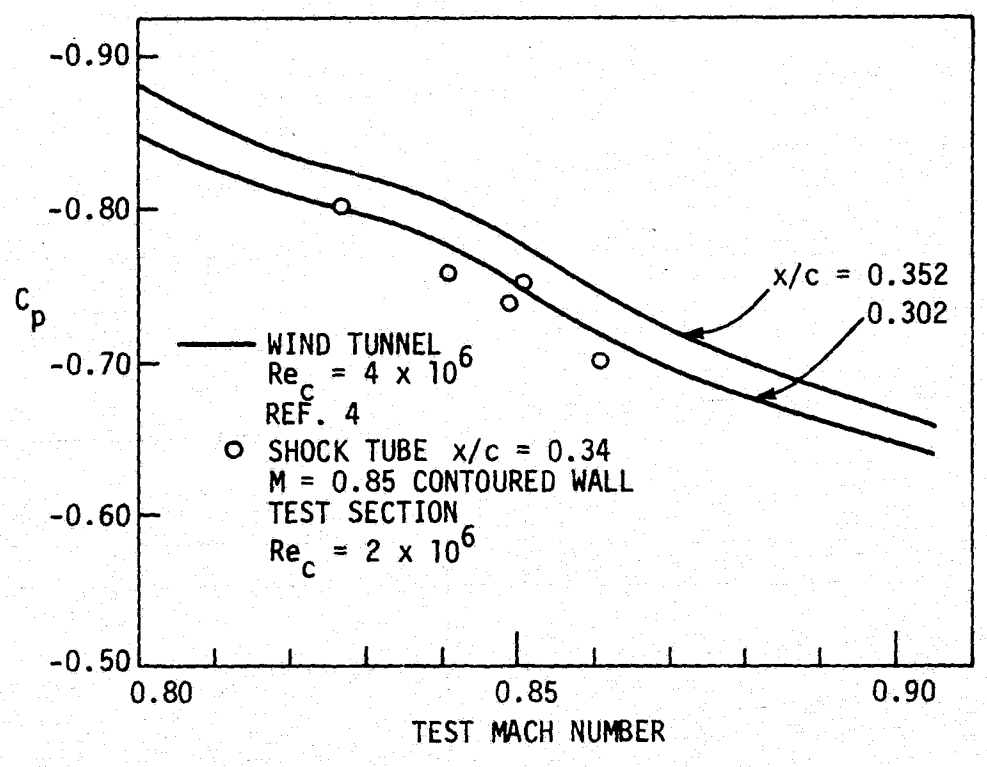

(b) Pressure coefficients vs test Mach Number.

Fig. 5. Concluded.

the quantities with the subscript ∞ were taken as those computed behind the primary shock, subscript 2. Figure 5(b) presents a comparison of C_p vs test Mach number for a typical case. It is seen that the shock tube results show the same trend as those measured in the wind tunnel, but do not quite agree with the wind tunnel results.

Figure 6 presents a comparison of pressure coefficients vs chord position obtained for the 0012 airfoil in the contoured wall test section and in the wind tunnel. A typical uncertainty interval for the present C_p values is shown. The shock tube results agree with the wind tunnel results near the airfoil leading edge and tend to disagree as the trailing edge is approached.

The results for the contoured wall tests in both Figures 4 and 6 indicate that the shock waves in the shock tube tests are displaced downstream of the corresponding shock waves observed in the wind tunnel. This suggests that the blockage has not been sufficiently alleviated by the wall contours used and that less confining walls are required.

In order to provide a more complete assessment of the contoured wall method of testing, the results obtained in [1] for the 12% thick circular arc airfoil using contoured walls will also be discussed. Wall contours for the circular arc airfoil study were based on the potential flow solutions of Murman and Cole [5] and Murman [6] for the circular arc airfoil.

Figure 7(a) presents for the circular arc airfoil a comparison of steady flow shock profiles measured from schlieren photos taken at various M_2 values using walls contoured for M = 0.85 with those determined from interferograms obtained by Wood and Gooderum [7] in a wind tunnel for a turbulent airfoil boundary layer flow upstream of the adverse pressure

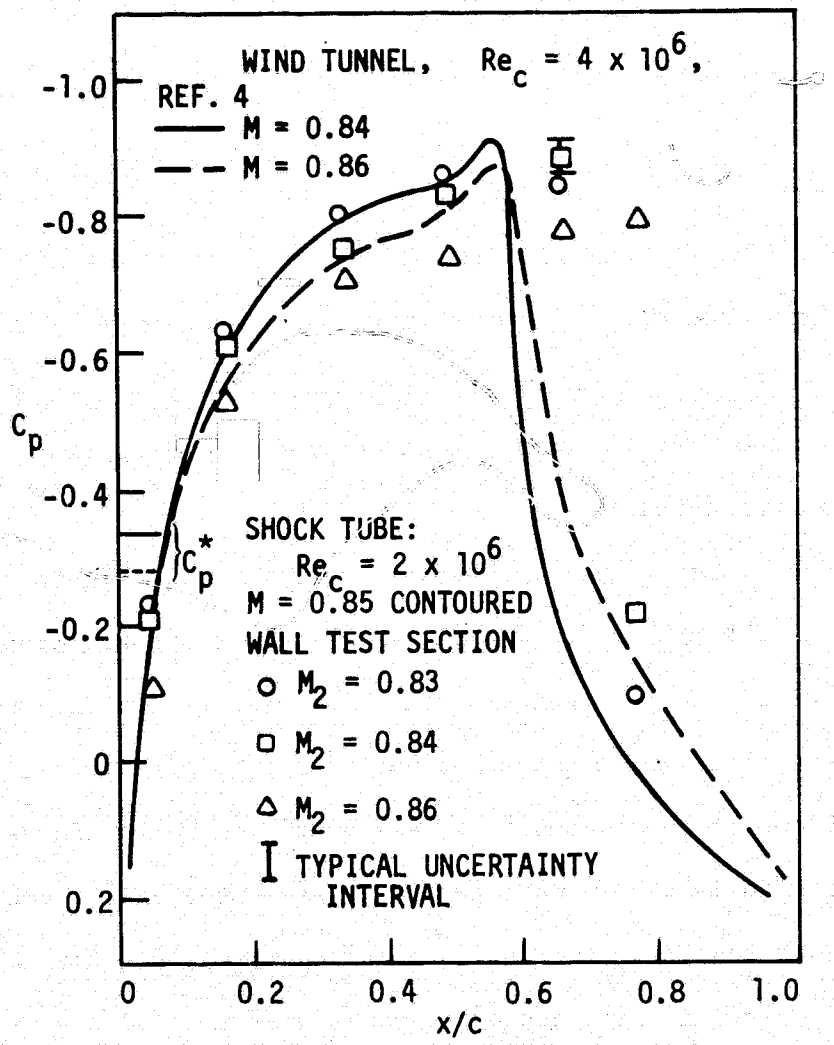

Fig. 6. Pressure coefficients vs chord position. NACA 0012 airfoil, $\alpha = 0$.

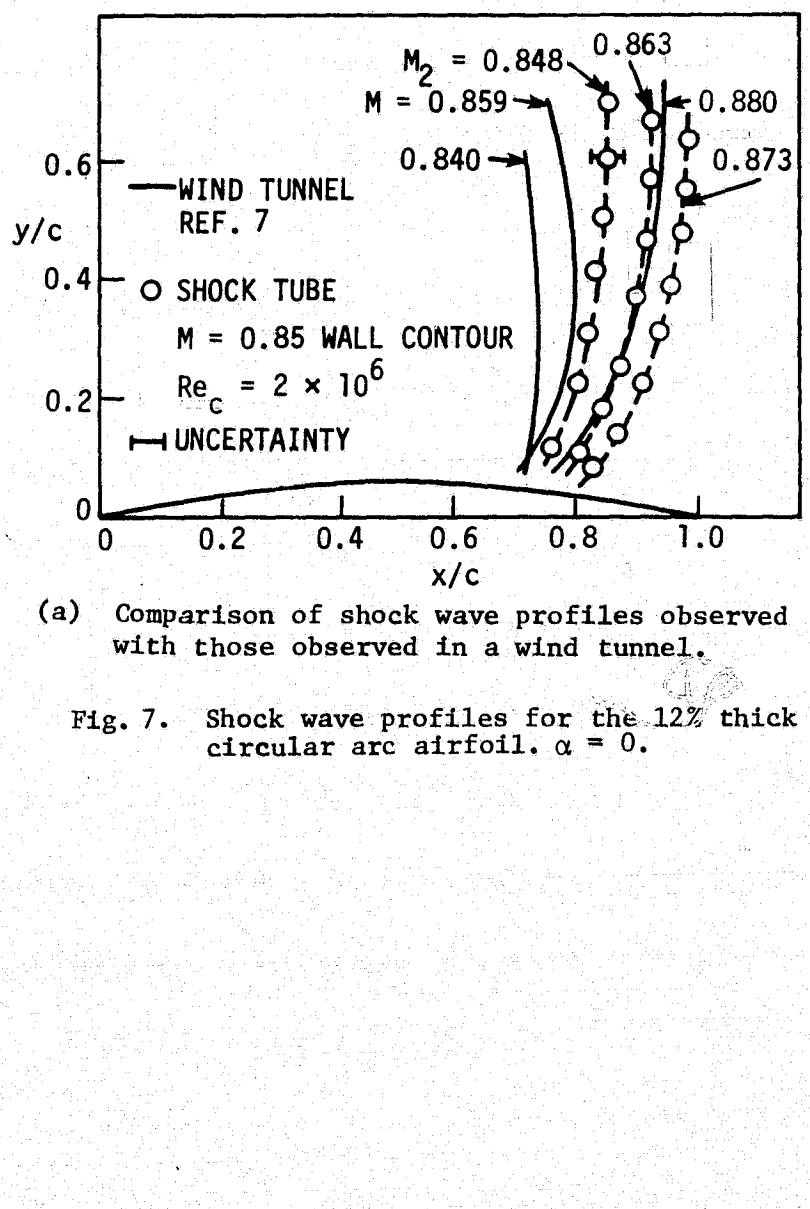

(a) Comparison of shock wave profiles observed with those observed in a wind tunnel.

Fig. 7. Shock wave profiles for the 12% thick circular arc airfoil. $\alpha = 0$.

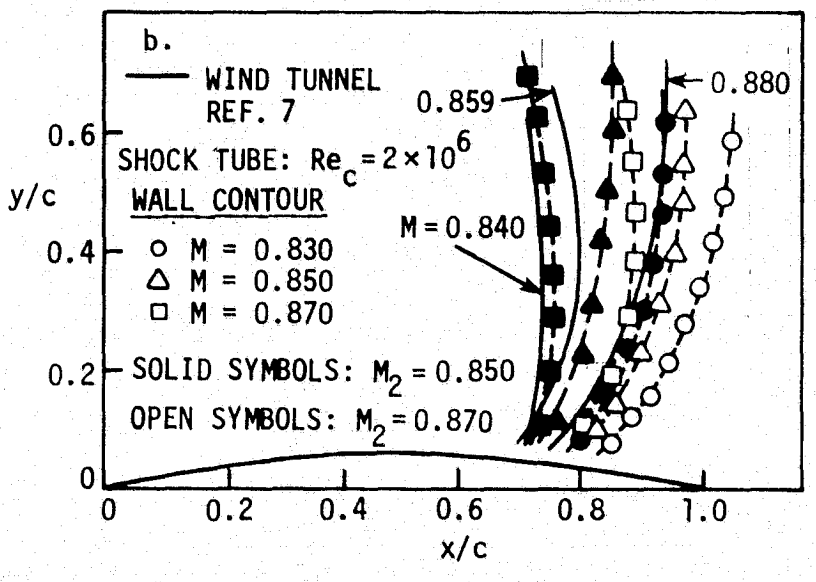

(b) Results showing the influence of wall contour on shock wave profiles.

Fig. 7. Concluded.

gradient region. The results presented here for the shock tube study of the circular arc airfoil differ somewhat from those in [1] in that primary shock wave attenuation has been taken into account (see Appendix A). An estimate of the typical uncertainty in shock position is shown in the figure. Figure 7(b) shows a similar comparison that permits the influence of wall contour to be assessed. It is seen from Fig. 7 that the shock profiles for the shock tube study exhibit fair agreement with wind tunnel results; the present profiles lie somewhat downstream of the expected positions at larger values of y/c. The results in Fig. 7(b) indicate that the shock tube results are somewhat sensitive to the wall contour.

Figure 8 presents a comparison of pressure coefficients C_p vs chord position determined from measured steady airfoil pressure values and those computed for the circular arc airfoil by the methods of [5] and [6]. (This comparison was made since wind tunnel pressure coefficients are not available at the test Mach and Reynolds numbers.) The uncertainties shown in the figure were determined from C_p values for various runs. The rather large uncertainty intervals were due to unavoidable roughness associated with the transducer mounting method which tended to produce scatter in the data. (The transducers were mounted in surface grooves and paraffin wax was used to fill voids and maintain the airfoil profile.) However, upstream of the shock wave boundary layer interaction, where the potential flow solution is expected to be applicable, the measured values agree well with the predicted curve.

The results for the contoured wall tests for the NACA 0012 airfoil in Figs. 4 and 6 and the circular arc airfoil in Figs. 7 and 8 depart somewhat from the corresponding wind tunnel results. Nonetheless, the

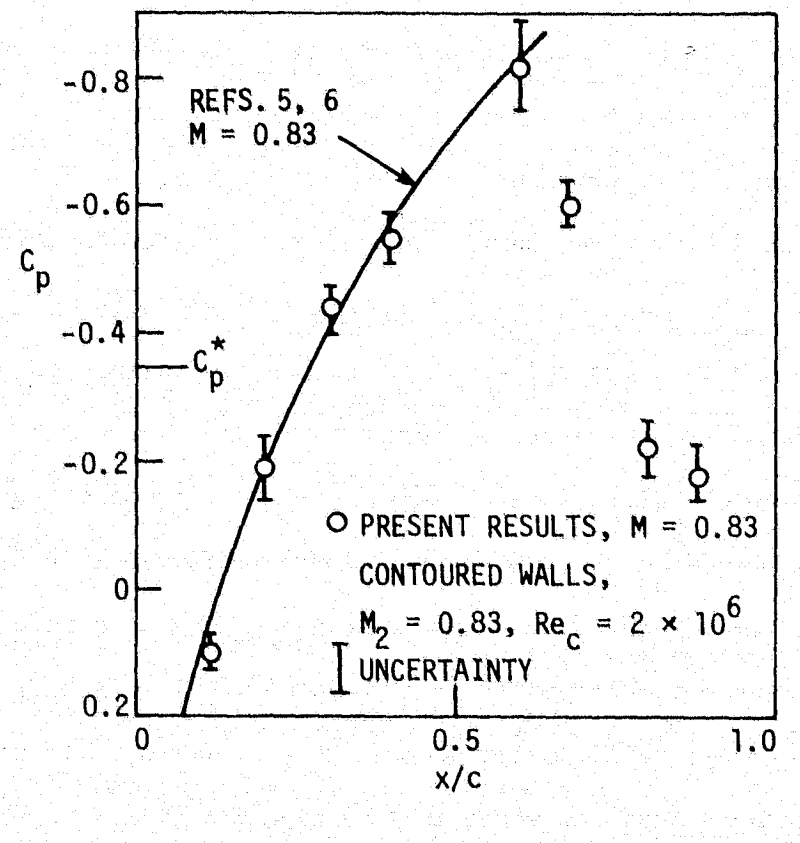

Fig. 8. Pressure coefficients vs chord position for the 12% thick circular are airfoil. $\alpha = 0$.

contoured wall method of testing does show that steady flows near to those observed in wind tunnels can be generated in shock tubes. The present results indicate that a different wall contour should be used for each airfoil profile tested. However, the contoured wall method of testing can provide test results, for which a flow boundary condition away from the airfoil is known, that are of use in analytical and numerical studies.

4. SLOTTED-WALL TEST SECTION STUDY

In order to provide testing flexibility, a shock tube slotted-wall test section similar to those used in wind tunnels to diminish wall interference effects has been developed. The objective was to provide a single test section that would accommodate various airfoil profiles and provide automatic flow compensation to minimize or eliminate wall effects. Although such test sections have been used extensively in transonic wind tunnels, they have not, to the author's knowledge, been used previously in aerodynamic testing in shock tubes.

Ventilated test sections for wind tunnels typically consist of walls with open areas and relatively large adjacent chambers which, when properly designed in combination, produce test section flows around models very near to those that would exist in free flight. Generally, the slotted-wall test section is preferred for subsonic flows and flows with Mach numbers slightly above unity, and therefore was the type chosen for development for transonic airfoil testing in the shock tube. Important differences exist between transonic flows in slotted-wall wind tunnels and those produced in shock tubes. As a result, slotted-wall wind tunnel design features could be used only as guides in the present study.

Figure 9 shows a diagram of the general features of the slotted-wall shock tube test section. As with the contoured-wall test section, an important feature related to the performance of the slotted-wall test section is the relative sizes of the airfoil and the test section. This is characterized by the ratios H/2c and A_f/A_{ts}. Additional considerations for the slotted-wall test section include the wall-slot

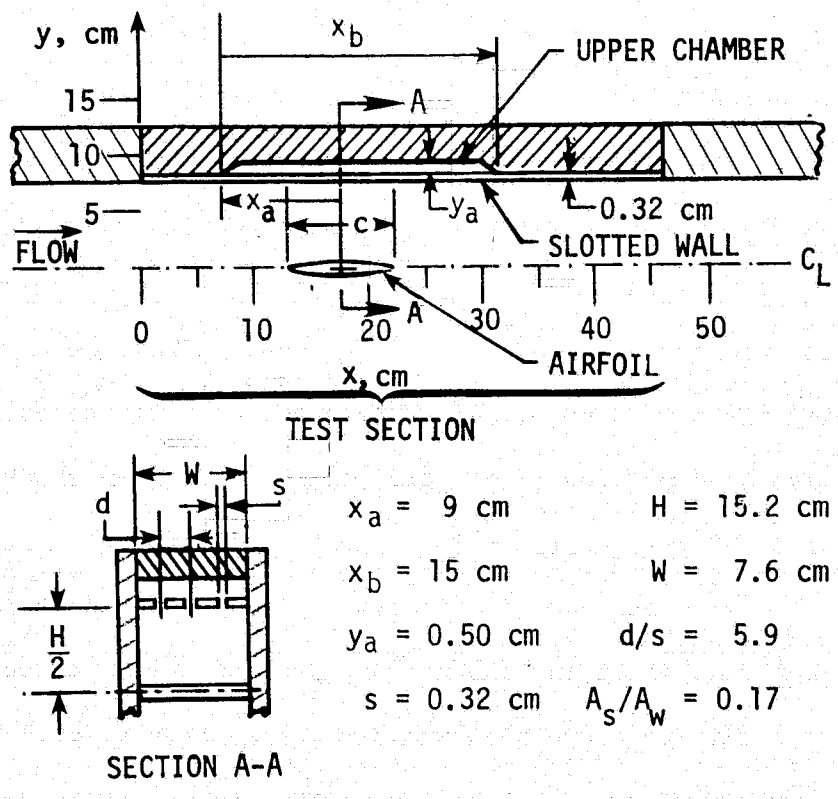

Fig. 9. Shock tube slotted-wall test section.

geometry and the chamber size and configuration. The latter factors influence the test section performance to a considerable extent. Centrifugal forces accompanying streamline curvature produced by the presence of the model produce flow through the slots into and out of the chambers and an associated regulating effect. It has been found for wind tunnels [8] that provided chamber size, slot spacing d/s, and the ratio of the slot area to the corresponding wall area A_s/A_w are chosen properly, the flow around the model will correspond to free flight flow, with departure from this flow being found to occur only in a narrow region adjacent to the wall, particularly in the vicinity of the slots. Values of A_s/A_w range up to 0.3 for various wind tunnels with slotted walls, and the number of slots varies according to the desired A_s/A_w and d/s. The slot width to the slotted-wall thickness is typically unity and larger. Chambers for wind tunnel test sections are usually relatively large (of the order of the test section volume). In view of the 3.5 ms testing time in the present study, the chamber volume (characterized by x_b, y_a, and W in Fig. 9) must be of such size that steady flow is attained in both the test section and in the chambers well within the testing time. Due to the differences between transonic testing in the wind tunnel and the shock tube, the present test section, Fig. 9, was designed to permit different combinations of variables affecting test section performance to be studied.

Flows over the 7.6 cm chord, 12% thick, circular arc airfoil (A_f/A_{ts} = 0.060, H/2c = 1.0) at zero angle of attack with a nominal Mach number 0.85 and a chord Reynolds number of 2×10^6 were studied for several different slot and chamber geometries. Results in terms of flow fields observed by schlieren photography were compared to corresponding results

obtained in the wind tunnel and the shock tube with contoured test section walls. Initially, tests were carried out with three slots per wall, each slot 0.32 cm in width, extending the length of the test section ($d/s = 7.9$, $A_s/A_w = 0.13$). Early tests with chamber volume one half the test section half-volume produced unsteadiness due to reflected waves in the chambers. Subsequent tests with reduced chamber volume, changes in chamber configuration, and 0.32 cm wide slots ranging in number from three to five per wall showed that steady flows of 2 ms duration could be produced within the 3.5 ms testing time. Further, it was determined that by proper choice of values for the controlling variables (chamber length, height, and position and the number of slots), airfoil flows for the circular arc airfoil close to those observed in the wind tunnel could be produced. The final configuration consisted of four 0.32 cm wide slots of effective length x_b and chambers with dimensions $x_a = 9$ cm, $x_b = 15$ cm, $y_a = 0.5$ cm and $W \simeq 7.6$ cm, yielding $A_s/A_w = 0.17$ and $d/s \simeq 5.9$ (see Fig. 9).

Figure 10(a) shows a typical schlieren photo taken at $t' = 2.5$ ms of the steady flow over the 7.6 cm chord length circular arc airfoil in the above-described slotted-wall test section. Figure 11 shows shock profiles for the 7.6 cm chord length circular arc airfoil obtained at three values of test Mach number. Also shown are the wind tunnel shock profiles and a shock profile observed at $M_2 = 0.85$ in the contoured-wall test section. The figure shows good agreement between the shock tube slotted-wall shock profiles for $c = 7.6$ cm and the wind tunnel shock profiles.

Figure 12 presents a comparison of pressure coefficients at five positions on the circular arc airfoil obtained using the slotted-wall

(a) 12% thick circular arc airfoil; c = 7.6 cm, M_2 = 0.86, α = 0.

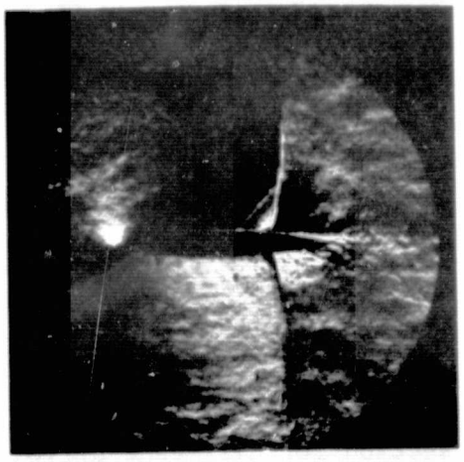

(b) 12% thick circular arc airfoil; c = 5.8 cm, M_2 = 0.86, α = 0.

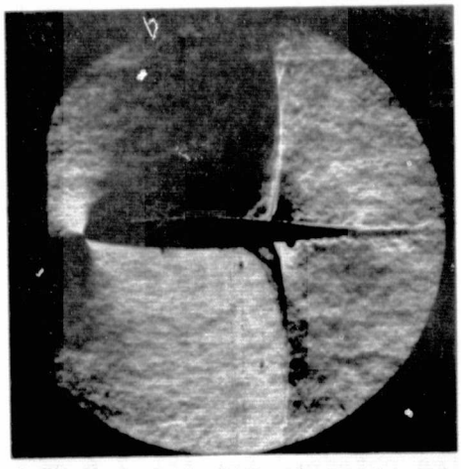

(c) NACA 64A010 airfoil; c = 7.6 cm, M_2 = 0.87, α = 0.

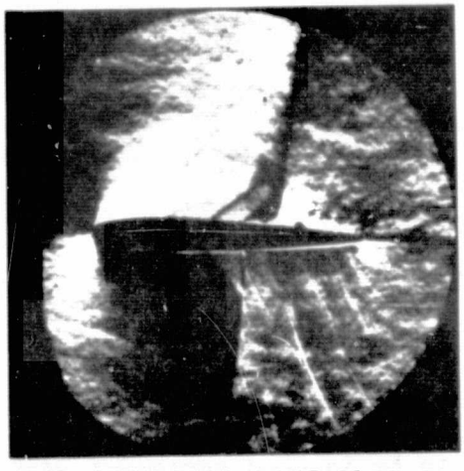

(d) NACA 0012 airfoil; c = 7.6 cm, M_2 = 0.85 α = 2°. Schlieren knife edge inverted.

Fig. 10. Schlieren photos of flows produced in the slotted-wall shock tube test section, Fig. 9. $Re_c = 2 \times 10^6$. t' = 2.5 ms.

test section at M_2 = 0.85 and corresponding measurements obtained under the same flow conditions using the same model in the contoured wall test section. The agreement is quite good. Thus, Figs. 11 and 12 indicate that flows near to those observed in the wind tunnel for the circular arc airfoil were produced in the slotted-wall test section described in Fig. 9.

In order to investigate the performance of the slotted-wall test section for different airfoil profiles, the following airfoils were also tested at zero angle of attack: a 12% thick circular arc with c = 5.8 cm, an NACA 64A010 and an NACA 0012, both with c = 7.6 cm. Study of the first two airfoils was limited to schlieren photography.

Testing the shorter chord circular arc airfoil in place of the 7.6 cm circular arc airfoil resulted in a change in H/2c from 1.0 to 1.31 and in A_f/A_{ts} from 0.060 to 0.046. Figure 10(b) shows a schlieren photo of the flow observed in the slotted-wall test section for the circular arc airfoil with c = 5.8 cm. Shock profiles for this airfoil for three values of M_2 are shown as the solid symbols in Fig. 11 and are observed to be in good agreement with both the profiles obtained for the 7.6 cm chord circular arc airfoil in the slotted-wall test section and wind tunnel profiles.

Testing the NACA 64A010 airfoil in the shock tube slotted-wall test section resulted in H/2c = 1.0 and A_f/A_{ts} = 0.050. Figure 10(c) is a schlieren photo of the flow for the 64A010 profile. Shock wave profiles for this airfoil for a range of Mach number and $Re_c \doteq 2 \times 10^6$ are compared in Fig. 13 with those observed in the Ames 2 x 2 ft wind tunnel by Stivers [4] at $Re_c = 4 \times 10^6$ using a 15.2 cm chord length model. For the

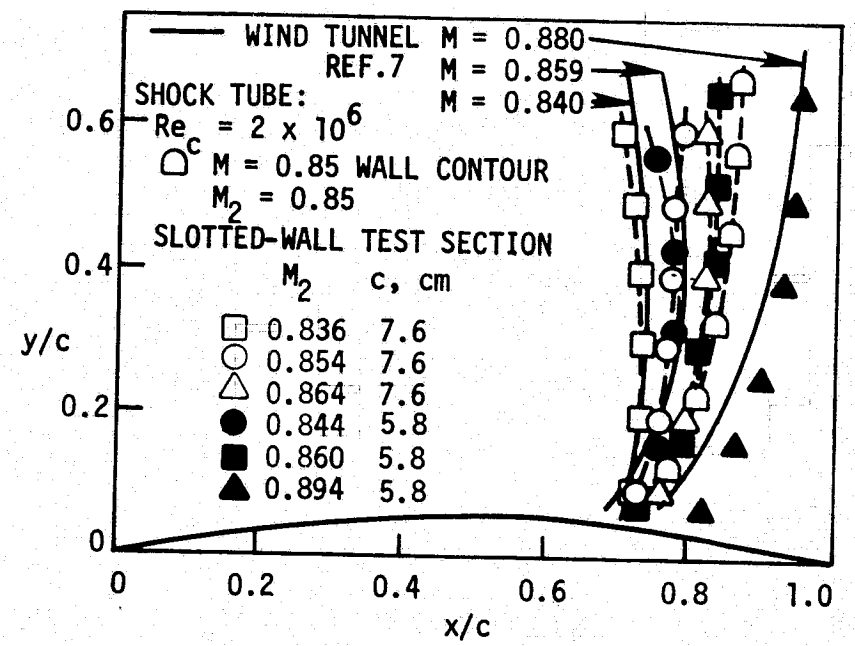

Fig. 11. Comparison of shock wave profiles for the circular are airfoil. $\alpha = 0$.

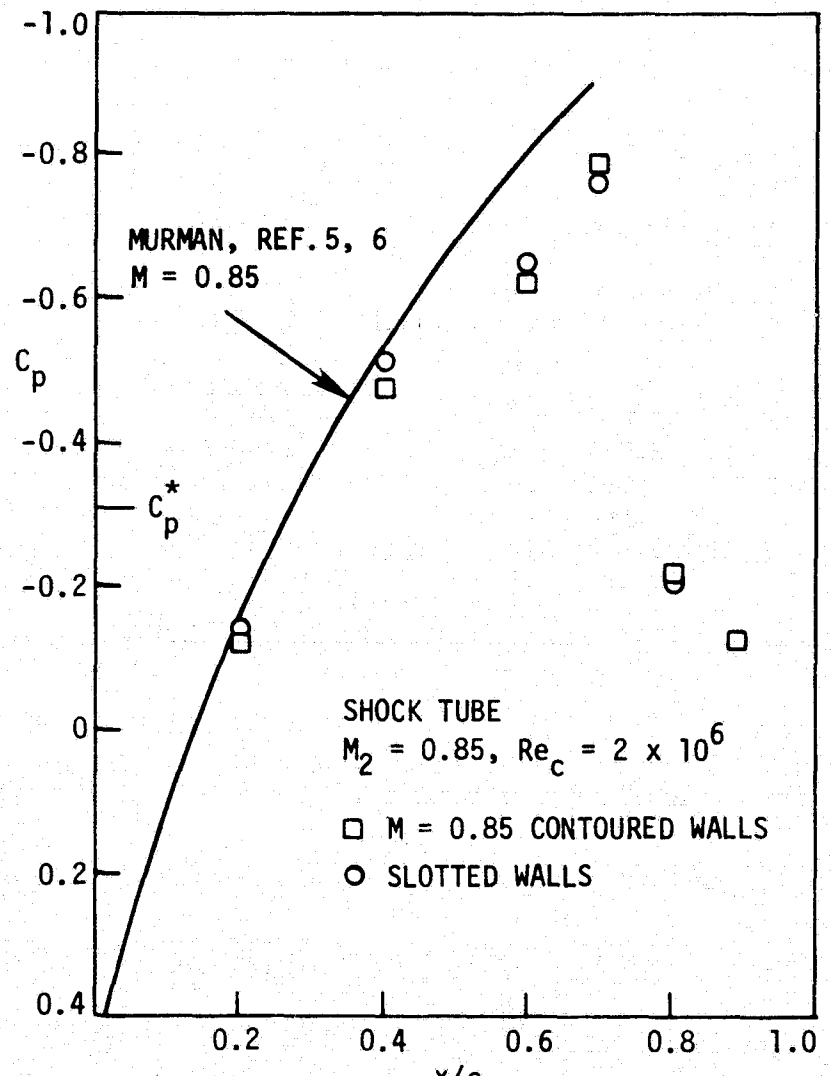

Fig. 12. Comparison of pressure coefficients for the circular are airfoil. $\alpha = 0$.

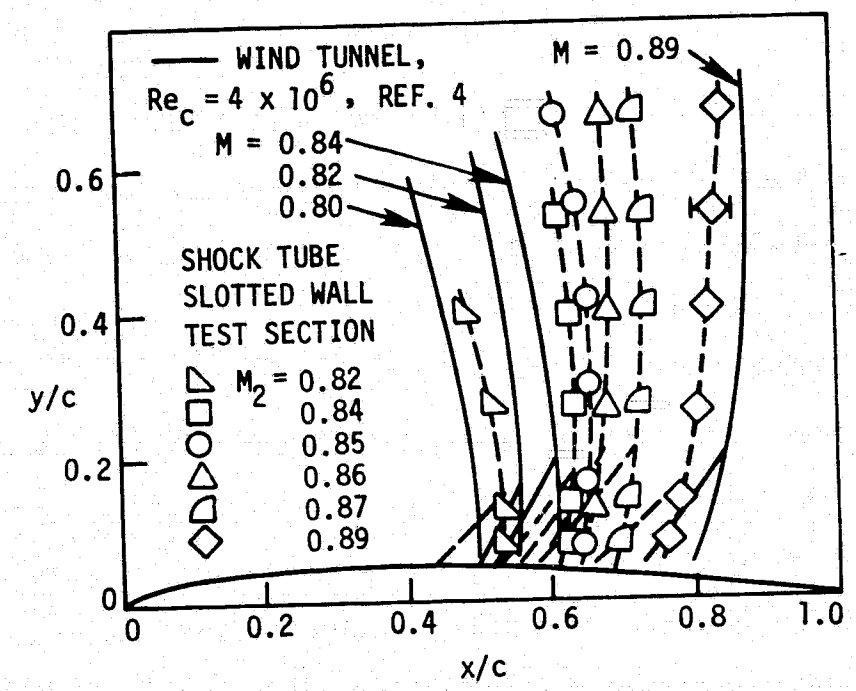

Fig. 13. Shock wave profiles for the NACA 64A010 airfoil. α = 0, Shock tube $Re_c = 2 \times 10^6$.

most part the agreement between the shock tube and the wind tunnel results is good. The present results reproduce the lambda shock configuration near the airfoil and show the same trends of variation of shock profile position with Mach number as do the results from the wind tunnel study.

Testing of the NACA 0012 airfoil in the slotted-wall test section was accomplished by using the same test airfoils that were used in the contoured wall tests of the 0012 profile. Figure 14 presents a comparison of the shock profiles obtained for the 0012 airfoil at zero angle of attack and the corresponding wind tunnel profiles. The agreement between the two sets of profiles is good for the complete range of Mach number.

Pressure coefficients vs chord position for the 0012 airfoil tested in the slotted wall test section are shown in Fig. 15 for three values of M_2. The results are essentially in agreement with the wind tunnel results for the forward half of the airfoil. Except for the one point for $M_2 = 0.87$ at $x/c = 0.66$, the C_p values toward the trailing edge tend to be slightly larger than those measured in the wind tunnel. The uncertainty intervals shown in Fig. 15 for the shock tube results at $M_2 = 0.85$ tend to be larger in the regions where C_p changes most rapidly with chord position. The uncertainty intervals shown are based on the analytical uncertainty analysis presented in [1] and on the range of the experimental data obtained at the given chord positions. It appears that the uncertainties in the shock tube data tend to be larger than for typical pressure coefficient measurements made in wind tunnels.

From the results in Figs. 11 to 15 it is seen that the shock tube slotted wall test section as described in Fig. 9 has produced good results for the different symmetric airfoil profiles tested at zero

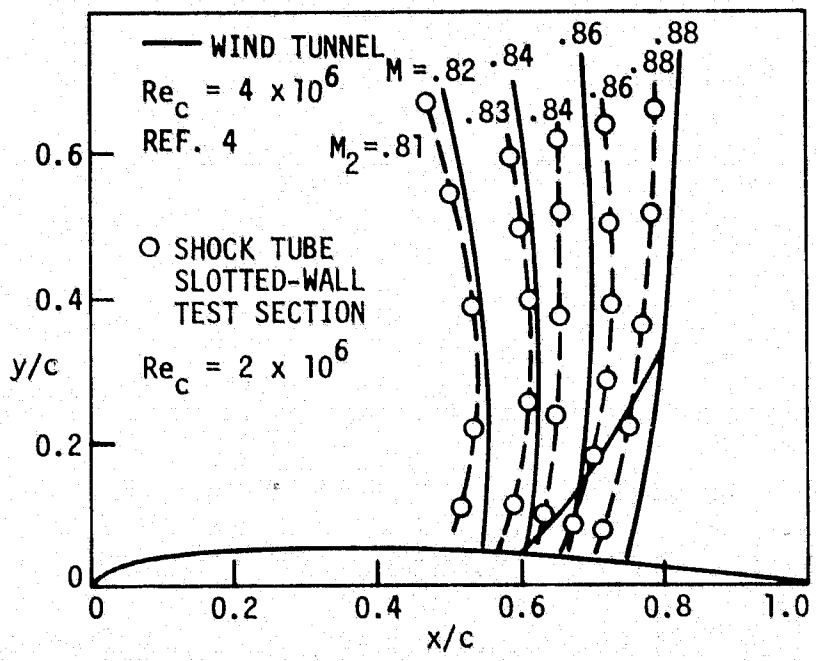

Fig. 14. Shock wave profiles for the NACA 0012 airfoil. $\alpha = 0$.

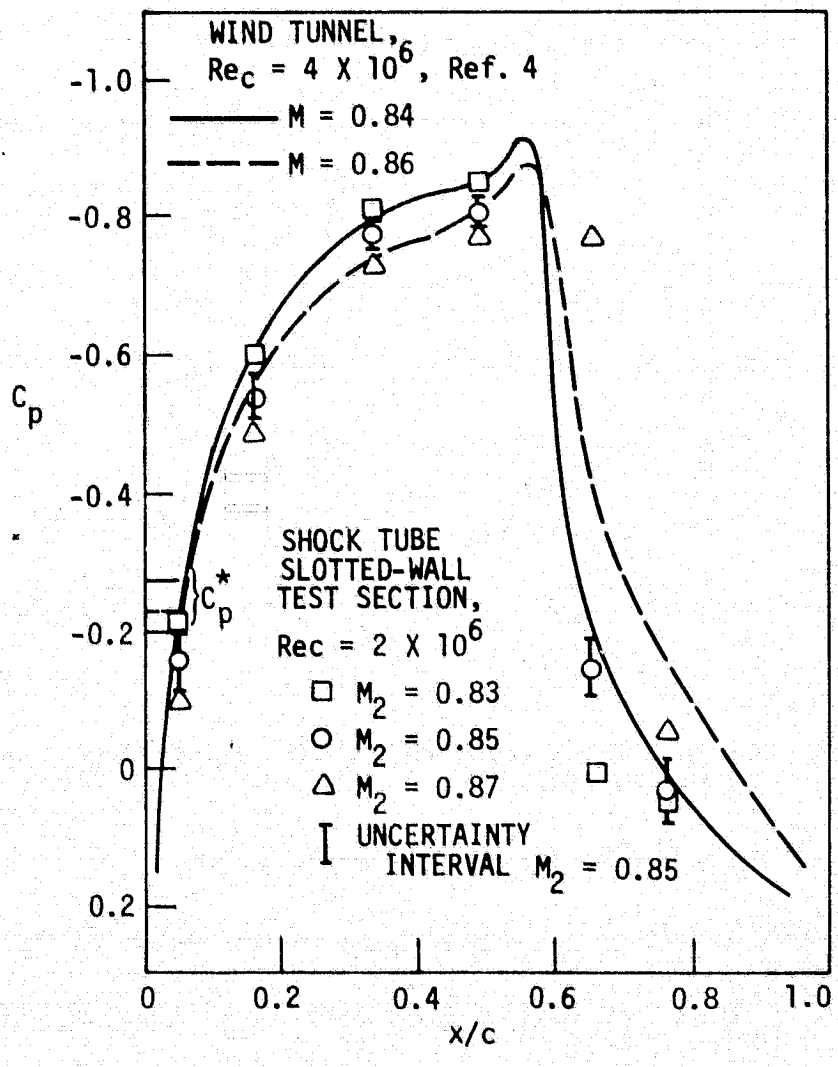

Fig. 15. Pressure coefficients vs chord position for the NACA 0012 airfoil. $\alpha = 0$.

angle of attack for test Mach numbers ranging from about 0.82 to about 0.89. It appears that the test section described in Fig. 9 is limited to this range. This is evidenced by the comparison of pressure coefficients in Fig. 16. This figure compares pressure coefficients for the NACA 0012 profile obtained using the shock tube slotted-wall test section with those measured by Amick [9] in a wind tunnel at a test Mach number of 0.75 and at about the same chord Reynolds number. It is seen that there is significant disagreement between the shock tube and wind tunnel results.

In order to investigate the performance of the slotted wall test section for non-symmetric flows, the 7.6 cm chord 0012 airfoil was studied at two degrees angle of attack. Figure 10(d) is a typical schlieren photo of the flow produced. Figure 17 presents a comparison of shock wave profiles obtained and those observed by Stivers [4] at $\alpha = 2^{o}$ in the Ames 2 x 2 ft wind tunnel. For the most part the agreement between the shock tube and wind tunnel results is good.

Pressure coefficients obtained for the 0012 profile at two degrees angle of attack in the slotted-wall test section are compared with corresponding wind tunnel results in Fig. 18 for three values of test Mach number. Two points from the shock tube study exhibit significant disagreement with the wind tunnel results. These are the point in Fig. 18(a) for the lower surface at $x/c = 0.49$ and the point in Fig. 18(c) for the lower surface at $x/c = 0.66$. Both of these points are in the immediate vicinity of the intersection of the shock wave and the airfoil profile. The remaining points in Fig. 18 are in fairly good agreement with the wind tunnel results.

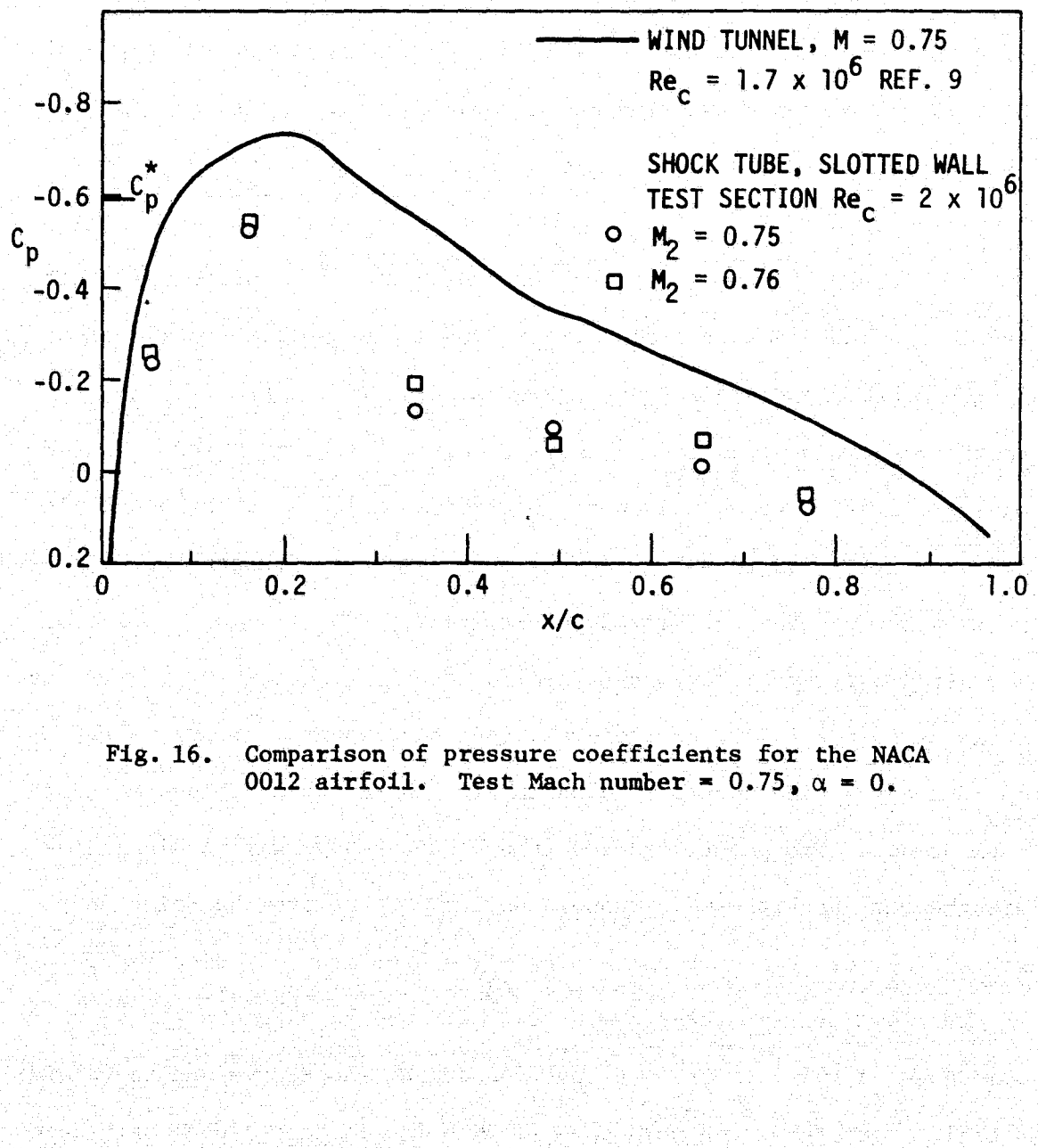

Fig. 16. Comparison of pressure coefficients for the NACA 0012 airfoil. Test Mach number = 0.75, α = 0.

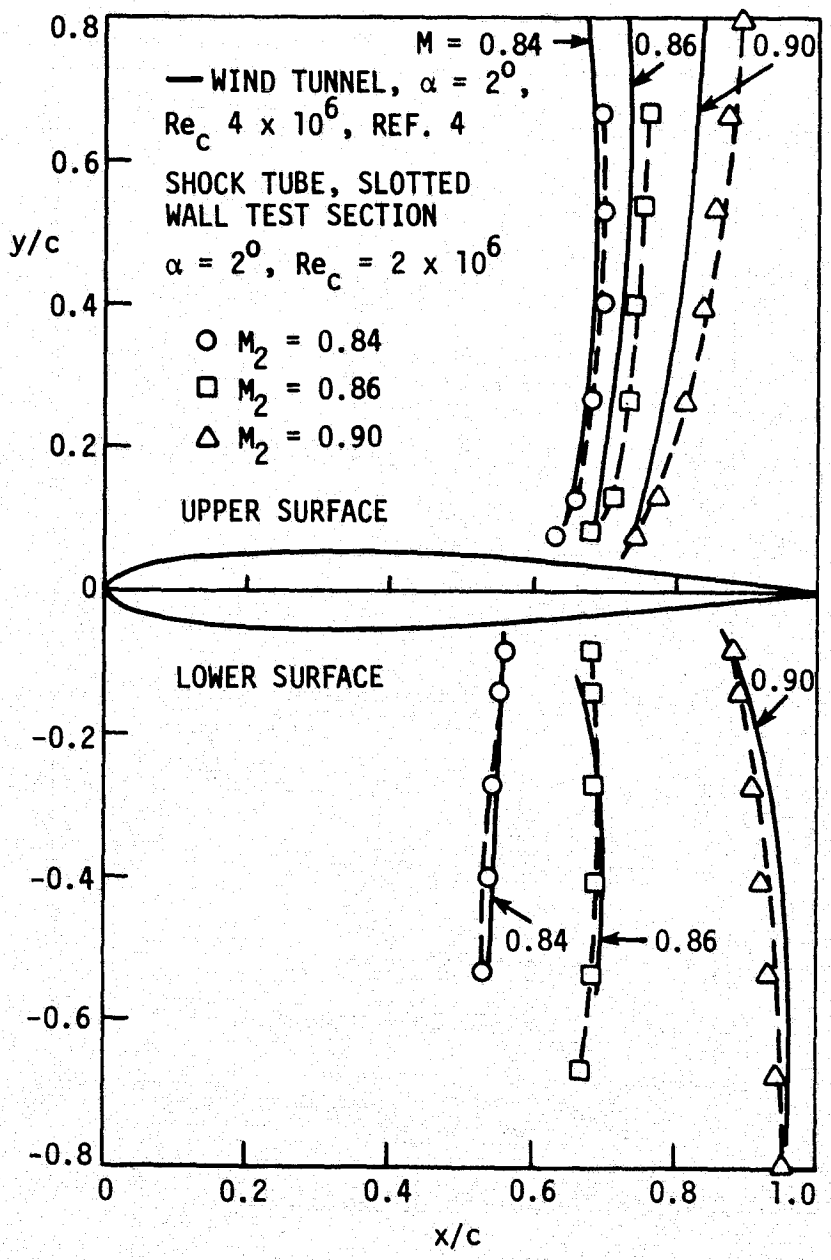

Fig. 17. Comparison of shock wave profiles for the NACA 0012 airfoil at two degrees angle of attack.

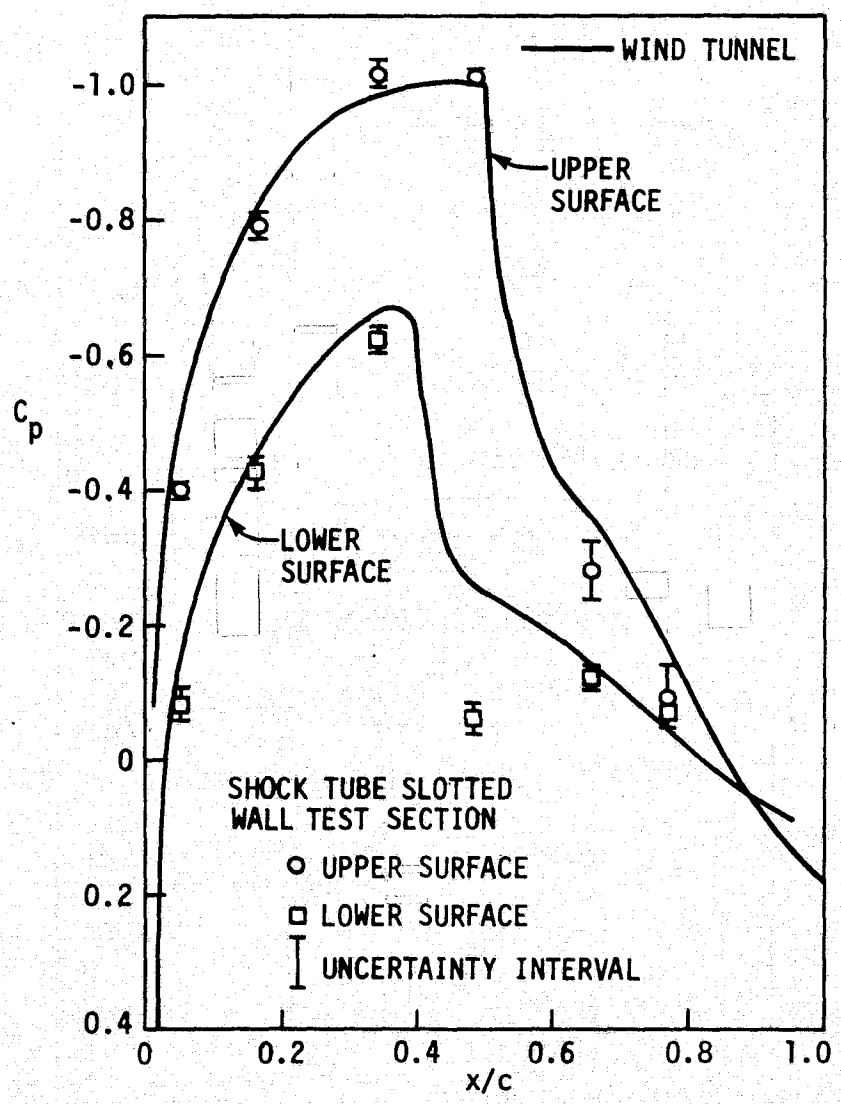

(a) Test Mach number = 0.819.

Fig. 18. Comparison of pressure coefficients for NACA 0012 airfoil profile at two degrees angle of attack for various Mach numbers. Wind tunnel $Re_c = 4 \times 10^6$ (Ref. 4). Shock tube $Re_c = 2 \times 10^6$.

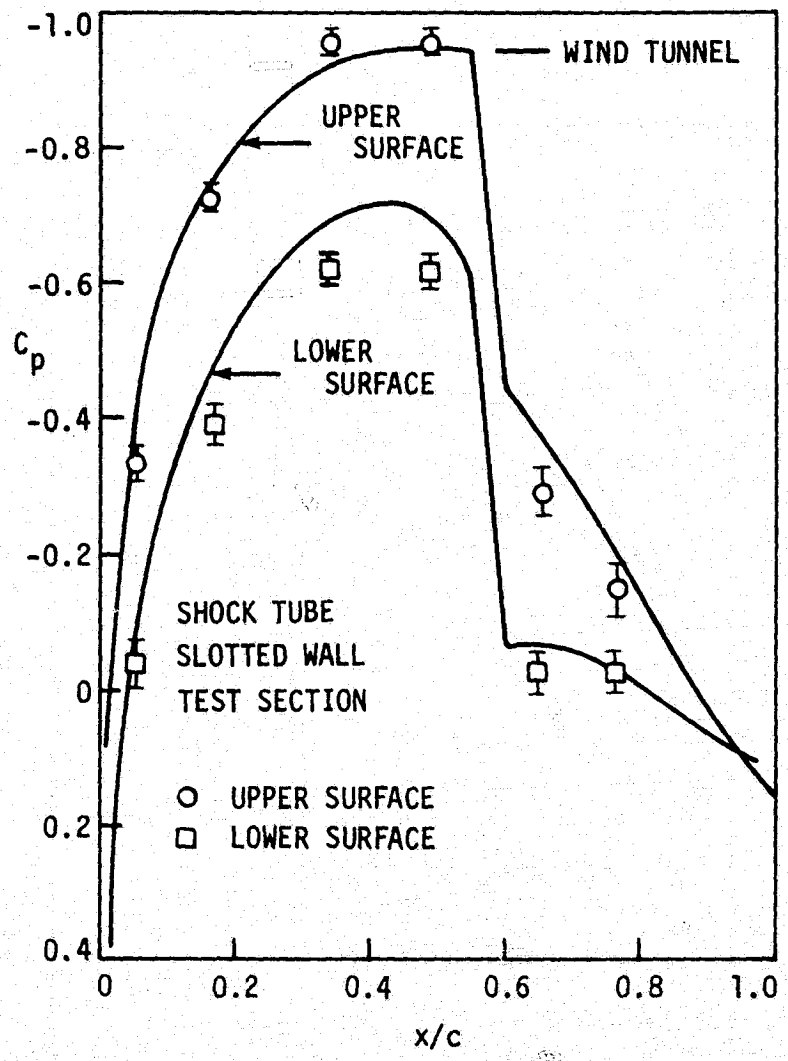

(b) Test Mach number = 0.842.

Fig. 18. Continued.

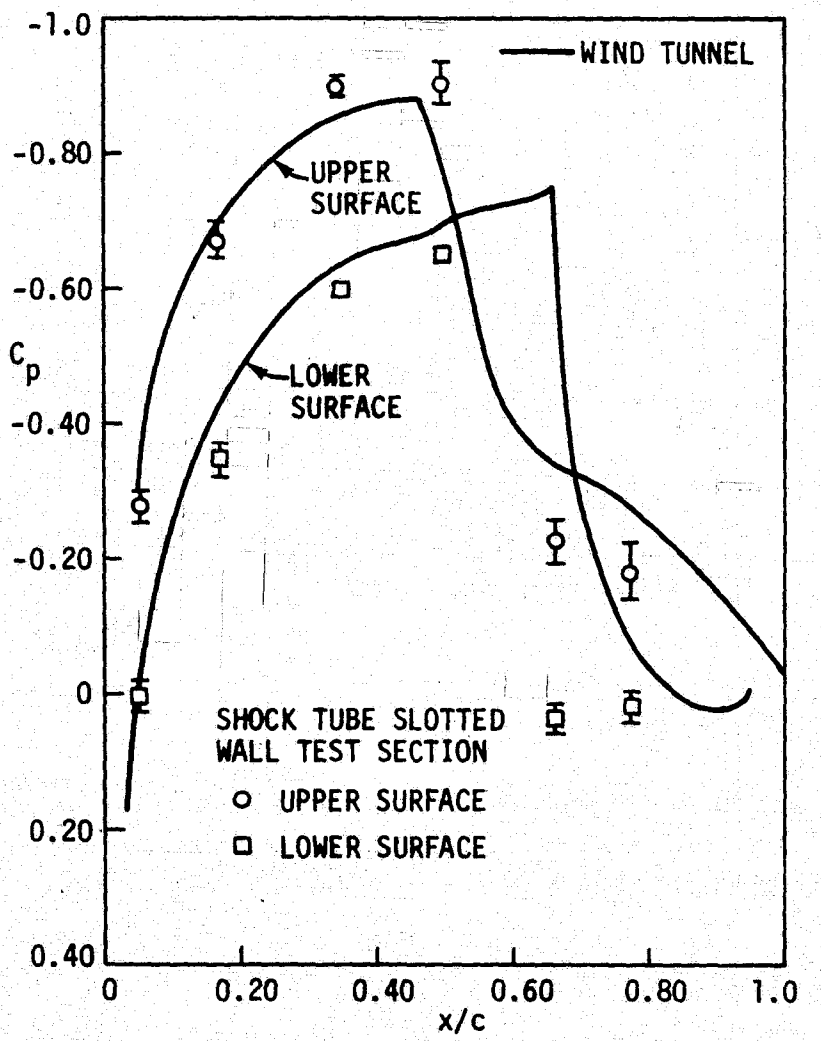

(c) Test Mach number = 0.860.

Fig. 18. Concluded.

The collective results obtained for the various airfoil tests in the shock tube slotted wall test section as presented in Figs. 11 to 18 indicate that the slotted wall test section described in Fig. 9 essentially exhibits the desired performance characteristics for test Mach numbers ranging from about 0.82 to about 0.89.

5. CONCLUDING REMARKS

This study has shown that the wall interference problem in a shock tube test section intended for steady two-dimensional transonic airfoil testing can be successfully dealt with by use of either a contoured wall test section or a properly-designed slotted-wall test section. Although the wall contouring method requires that contours be matched to each airfoil tested and may not produce flows that are in all respects correct, the method does have the advantage of producing test flows with known boundary conditions. Thus, it can provide reference flows useful in analytical and numerical studies. The fixed-geometry slotted-wall test section developed in this study produces essentially correct airfoil flows for Mach numbers in the approximate range $0.82 \leq M_2 \leq 0.89$ at $Re_c = 2 \times 10^6$, and exhibits good testing flexibility, as evidenced by good agreement found for several cases between shock tube generated airfoil flows and corresponding airfoil flows observed in conventional wind tunnels.

The results of this study provide further evidence that the shock tube is a viable alternate facility for studying transonic airfoil flows at high Reynolds numbers.

6. ACKNOWLEDGMENTS

This research was supported by the Engineering Research Institute of Iowa State University through funds provided by NASA-Ames (Grant NSG-2152).

The assistance rendered by Michael J. Chaney, a mechanical engineering graduate student, in conducting the experimental work associated with this research is gratefully acknowledged.

7. REFERENCES

1. Cook, W. J., Chaney, M. J., Presley, L. L., and Chapman, G. T., "Application of shock tubes to transonic airfoil testing," NASA TP 1268, April, 1978.
2. Cook, W. J., Presley, L. L., and Chapman, G. T., "Use of shock tubes in high Reynolds number transonic testing," Proceedings of the Tenth International Shock Tube Symposium, Kyoto, Japan, 1975, pp. 472-479.
3. Arieli, R., NASA Ames Research Center, private communication.
4. Stivers, L. S., Jr., NASA Ames Research Center, private communication.
5. Murman, E. M., and Cole, J. D., "Calculation of plane steady transonic flows," AIAA J., Vol. 9, No. 1, Jan. 1971, pp. 114-121.
6. Murman, E. M., "Analysis of embedded shock waves calculated by relaxation methods," AIAA J., Vol. 12, No. 5, May 1974, pp. 626-633.
7. Wood, G. P., and Gooderum, P. B., "Investigation with an interferometer of the flow around a circular-arc airfoil at Mach numbers between 0.6 and 0.9," NACA TN 2801, 1952.
8. Goethert, B. H., Transonic wind tunnel testing, Pergamon Press, New York, 1961.
9. Amick, J. L., "Comparison of the experimental pressure distribution on an NACA 0012 profile at high speeds with that calculated by the relaxation method," NACA TN 2174, 1950.

8. APPENDIX A

EFFECT OF SHOCK WAVE ATTENUATION

It is a well-known fact that the speed of the primary shock wave decreases as the shock wave propagates down the driven section of the shock tube. Thus, the shock wave path in the t-x diagram (Fig. 1) curves slightly upward in real shock tube flows. This attenuation in wave speed produces a small variation with time in the incoming flow relative to the airfoil in the test section of the shock tube. This variation was taken into account in the present shock tube application.

8.1 Attenuation Measurements

Two methods of determining shock wave attenuation were used in the present study. First, the decrease in shock speed was directly measured. Second, the variation of pressure with time was measured at the test section location, and shock wave attenuation was inferred from this measurement.

Figure A.1 presents a schematic diagram of the arrangement used to directly measure shock wave attenuation. Measurement of the time required for the shock to travel the distance intervals Δx_{ab} and Δx_{cd} privide quantitative information to establish the approximate attenuation. The difference in $U_{s,ab} = \Delta x_{ab}/\Delta t_{ab}$ and $U_{s,cd} = \Delta x_{cd}/\Delta t_{cd}$ divided by the length 3.962 m yields an approximate attenuation per unit length of driven tube. The shock speed for the airfoil tests at nominal conditions in this study, $M_2 = 0.85$ and $Re_c = 2 \times 10^6$, was 0.6285 mm/μs. For the typical distance $\Delta x = 0.305$ m (Fig. A.1), the corresponding time interval

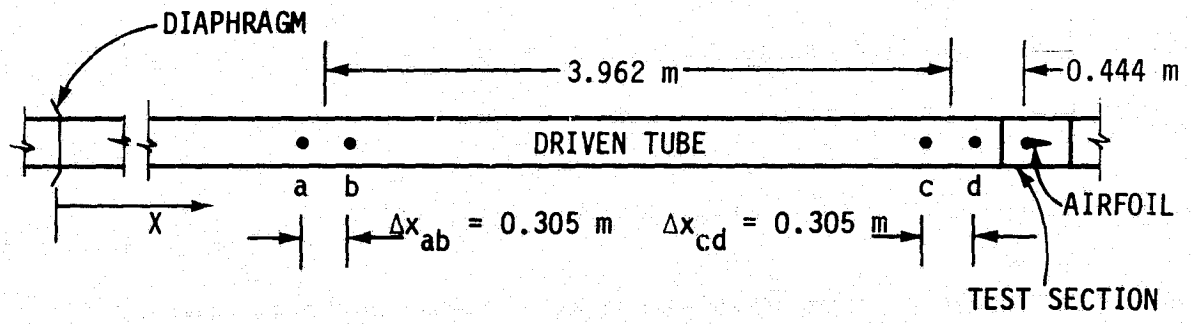

Fig. A.1. Arrangement and nomenclature for shock wave attenuation measurements.

Δt = 485 μs. A series of runs performed at M_2 = 0.85 and at conditions corresponding to $Re_c = 2 \times 10^6$ without an airfoil mounted in the test section showed that the shock speed at position ab was 0.0098 ± 0.0027 mm /μ s greater than that at position cd. Thus, the measured decrease in U_s per unit length of driven tube was 0.0098/3.962 = 0.0025 (mm/μs)/m.

Shock speed attenuation should produce a rise with time in the pressure p_2 at any given section in the driven tube. This might be expected to occur because free-stream gas particles initially located well upstream of the section are overtaken by a stronger shock than are those nearer to the section. The expected pressure increase with time has been measured and is illustrated in the graph of absolute pressure p_2 vs time in Fig. A.2. This figure is based on measurements of p_2 made using a Kulite pressure transducer positioned at x_d in Fig. A.1., flush with the sidewall to measure the wall static pressure. In Fig. A.2 t_g = 0 when the primary shock wave arrives at the gage. The change in p_2 over the nominal 3.5 ms testing time is about three percent. The measured variation of pressure with time can be used to estimate shock wave attenuation, provided the simplifying assumption is made that gas particles retain the pressure they attained on being overtaken by the shock wave. This can be illustrated using Fig. A.3 which shows the t-x diagram in the vicinity of a pressure transducer located at x_d in Fig. A.1.

A gas particle initially positioned at x_p arrives at the gage location at $t_g = t_{g,p}$. A gas particle initially at $x_{p'}$ is overtaken by a weaker shock and arrives at the gage location at time $t_{g,p'}$; earlier than a gas particle initially located at x_p. If the shock speed is known as a function of position upstream of the gage, and p_1 is known, the pressure

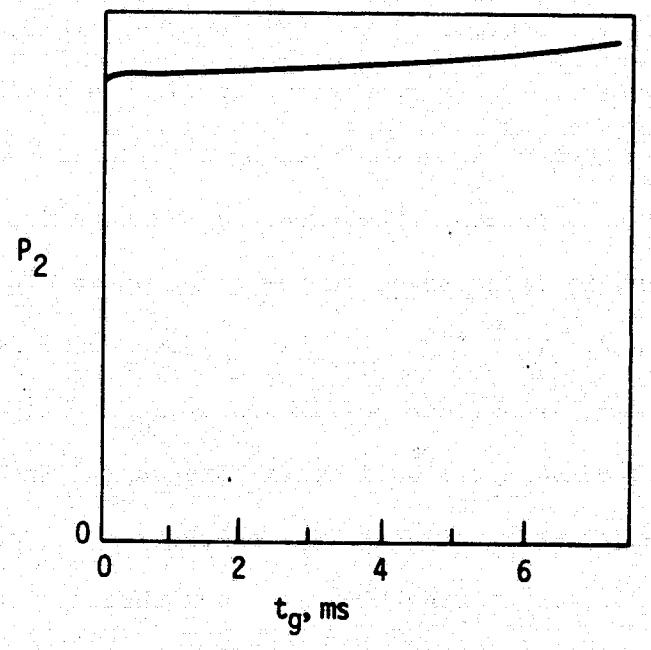

Fig. A.2. Measured absolute pressure p_2 vs time.

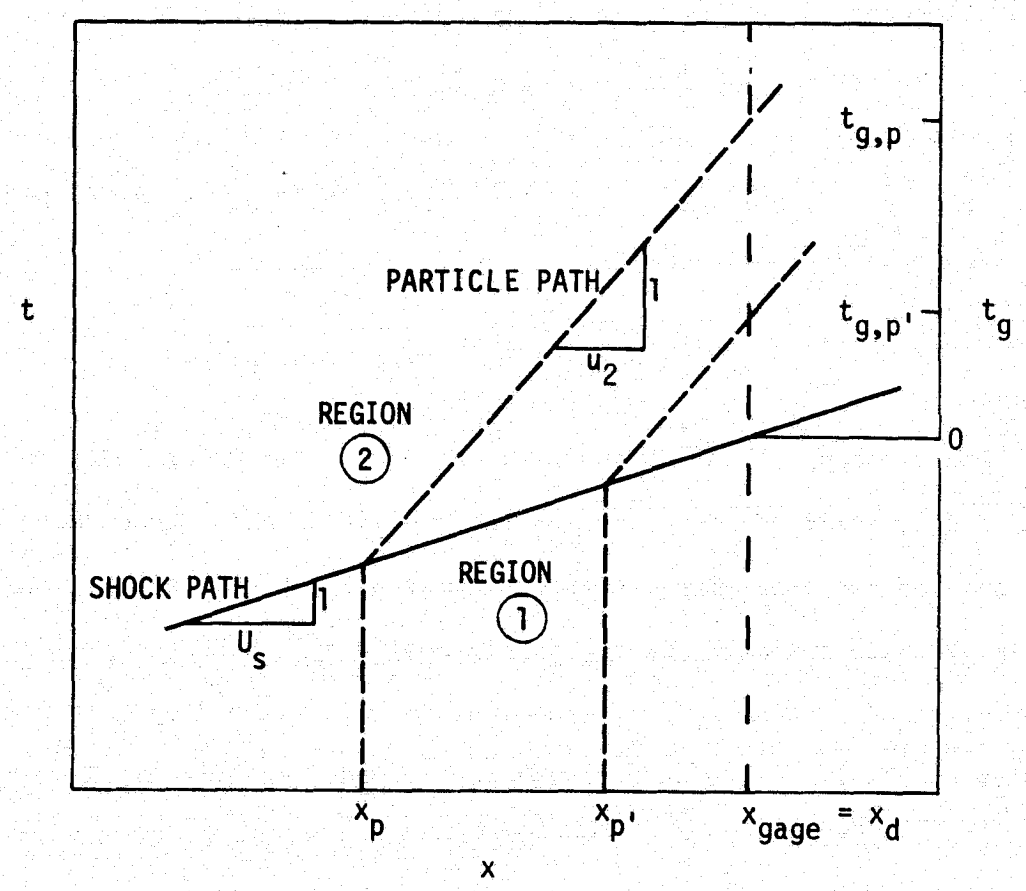

Fig. A.3. Time - distance diagram for the vicinity of location x_d, Fig. A.1.

at the gage location could be predicted provided it is also assumed that u_2 is locally constant. Conversely, if the pressure as a function of t_g is known, as in Fig. A.2, and the assumptions are retained, the shock speed as a function of position upstream of the gage can be approximated. Computations based on the above for two pressure records produced the following values for shock attenuation per unit length: 0.0028 (mm/μs)/m and 0.00394 (mm/μs)/m. Considering the approximations made, these values are in fair agreement with the value of 0.0025 (mm/μs)/m obtained from shock speed measurements.

8.2 Influence of Attenuation on Results

With the approximate attenuation in shock speed determined, there remains the matter of how to incorporate the attenuation into the data analysis. For the results presented in the body of this report, shock speeds were determined by appropriately modifying shock speeds measured at location cd in Fig. A.1. Steady flow was established by $t' \simeq 2$ ms. In view of this, all pressure transducer records for airfoil flows were read at $t' = 2.5$ ms.

Computations based on the method outlined above indicate that gas particles at the airfoil location at $t' = 2.5$ ms had as their origin a position 2.07 m upstream of the airfoil. Thus, use of a shock speed for data reduction measured at location cd in Fig. A.1 (0.444 m upstream of the airfoil) does not yield the correct p_2 or the correct M_2 for the incoming flow to the airfoil at $t' = 2.5$ ms. According to the above assumptions, the shock speed should have been measured at a location centered about a point 2.07 m upstream of the airfoil. Use can be made

of shock attenuation results to compute the shock speed and hence the time interval Δt_{cd} necessary to yield the appropriate values of p_2 and M_2 at the test section at $t' = 2.5$ ms. The distance 2.07 - 0.444 = 1.63 m multiplied by the shock attenuation per unit length yields the shock speed increment that must be added to the shock speed determined from measurements at location cd. Use of the values 0.0025 and 0.00394 (mm/μs)/m for shock attenuation and a value for shock speed of 0.6285 mm/μs determined at location cd yields corresponding adjusted shock speeds of 0.6323 and 0.6348 mm/μs. These values can be obtained by subtracting 4 ± 1 μs from Δt_{cd} (485 μs) that yields the shock speed 0.6285 mm/μs.

The results presented herein were determined by reducing the measured values of Δt_{cd} by 4 μs. Table A.1 shows the influence of this correction on results obtained for a typical run. It is seen that the influence of shock wave attenuation is small but significant, at least with respect to Mach number.

Table A.1. Example of influence of shock wave attenuation on experimental results: 7.6 cm chord NACA 0012 airfoil, $Re_c = 2 \times 10^6$, $T_1 = 308$ K.

Quantity	Results Without Considering Attenuation	Results Considering Attenuation
Δt_{cd}	485 μs	481 μs
M_2	0.850	0.860
C_p at x/c = 0.06	-0.180	-0.206
C_p at x/c = 0.34	-0.762	-0.765